PHYSICAL REVIEW D **95,** 114005 (2017)

Open-flavor charm and bottom $sq\bar{q}\bar{Q}$ and $qq\bar{q}\bar{Q}$ tetraquark states

Wei Chen,[1] Hua-Xing Chen,[2,*] Xiang Liu,[3,4,†] T. G. Steele,[1,‡] and Shi-Lin Zhu[5,6,7,§]

[1]*Department of Physics and Engineering Physics, University of Saskatchewan, Saskatoon, Saskatchewan, S7N 5E2 Canada*
[2]*School of Physics and Beijing Key Laboratory of Advanced Nuclear Materials and Physics, Beihang University, Beijing 100191, China*
[3]*School of Physical Science and Technology, Lanzhou University, Lanzhou 730000, China*
[4]*Research Center for Hadron and CSR Physics, Lanzhou University and Institute of Modern Physics of CAS, Lanzhou 730000, China*
[5]*School of Physics and State Key Laboratory of Nuclear Physics and Technology, Peking University, Beijing 100871, China*
[6]*Collaborative Innovation Center of Quantum Matter, Beijing 100871, China*
[7]*Center of High Energy Physics, Peking University, Beijing 100871, China*

(Received 10 February 2017; published 8 June 2017)

We provide comprehensive investigations for the mass spectrum of exotic open-flavor charmed/bottom $sq\bar{q}\bar{c}$, $qq\bar{q}\bar{c}$, $sq\bar{q}\bar{b}$, $qq\bar{q}\bar{b}$ tetraquark states with various spin-parity assignments $J^P = 0^+, 1^+, 2^+$ and $0^-, 1^-$ in the framework of QCD sum rules. In the diquark configuration, we construct the diquark-antidiquark interpolating tetraquark currents using the color-antisymmetric scalar and axial-vector diquark fields. The stable mass sum rules are established in reasonable parameter working ranges, which are used to give reliable mass predictions for these tetraquark states. We obtain the mass spectra for the open-flavor charmed/bottom $sq\bar{q}\,\bar{c}$, $qq\bar{q}\,\bar{c}$, $sq\bar{q}\,\bar{b}$, $qq\bar{q}\,\bar{b}$ tetraquark states with various spin-parity quantum numbers. In addition, we suggest searching for exotic doubly-charged tetraquarks, such as $[sd][\bar{u}\,\bar{c}] \to D_s^{(*)-}\pi^-$ in future experiments at facilities such as BESIII, BelleII, PANDA, LHCb, and CMS, etc.

DOI: 10.1103/PhysRevD.95.114005

I. INTRODUCTION

During the past 14 years, there are many unexpected hadrons observed experimentally, such as the XYZ states [1] and hidden-charm pentaquarks [2], etc. These resonances cannot be interpreted as conventional quark-antiquark mesons or three-quark baryons in the conventional quark model [3]. They are exotic hadron candidates, whose significant experimental and theoretical progress have been reviewed in Refs. [4–7].

Very recently, the D0 Collaboration reported the evidence for the narrow structure $X(5568)$ in the $B_s^0\pi^\pm$ invariant mass spectrum with 5.1σ significance [8]. Its mass and decay width were measured to be $m_{X(5568)} = 5567.8 \pm 2.9(\text{stat})^{+0.9}_{-1.9}(\text{syst})$ MeV and $\Gamma_{X(5568)} = 21.9 \pm 6.4(\text{stat})^{+5.0}_{-2.5}(\text{syst})$ MeV, and its spin-parity quantum number was determined to be either $J^P = 0^+$ or 1^+. Later, the LHCb and CMS collaborations also performed their analyses of the pp collision data at energies $\sqrt{s} = 7$ TeV and 8 TeV to search for the $X(5568)$ state [9,10], but they did not find any unexpected structure in the $B_s^0\pi^\pm$ invariant mass distribution. However, the D0 Collaboration themselves confirmed the $X(5568)$ meson in the $B_s^0\pi^\pm$ invariant mass distribution with another channel $B_s^0 \to D_s\mu\nu$ at the same mass and at the expected width and rate [11].

Reported in the $B_s^0\pi^\pm$ final states, the $X(5568)$ meson, if it exists, could be a bottom-strange $su\bar{d}\,\bar{b}$ (or $sd\bar{u}\,\bar{b}$) tetraquark state with valence quarks of four different flavors. To date, the $X(5568)$ resonance has trigged many theoretical studies, including the diquark-antidiquark tetraquark state [12–30], hadron molecule [31–38], nonresonant schemes [39], hybridized tetraquark model [40], and so on. One can find the detailed introduction for these theoretical studies in the recent review paper [41].

In the charm sector, the two narrow charm-strange mesons $D_{s0}^*(2317)$ and $D_{s1}(2460)$ were observed in 2003 in the $D_s^+\pi^0$ and $D_s^{*+}\pi^0$ invariant mass distributions by the *BABAR* [42] and CLEO [43] collaborations, respectively. Their observed masses are (2317.7 ± 0.6) MeV and (2459.5 ± 0.6) MeV, respectively, which are much lower than the Godfrey-Isgur (GI) model predictions [44]. These states quickly attracted many theoretical studies involving various exotic assignments [45,46], which can also be found in the review paper Ref. [41] and its related references. Among these configurations, the four-quark assignment $cq\bar{s}\,\bar{q}$ is particularly interesting.

Inspired by the experimental information and theoretical studies of the $X(5568)$, $D_{s0}^*(2317)$ and $D_{s1}(2460)$ mesons, we shall provide comprehensive studies for the open-flavor

*hxchen@buaa.edu.cn
†xiangliu@lzu.edu.cn
‡tom.steele@usask.ca
§zhusl@pku.edu.cn

charmed/bottom $sq\bar{q}\,\bar{Q}$ and $qq\bar{q}\,\bar{Q}$ tetraquark states in this paper. If the existence of the $X(5568)$ is confirmed, many other charmed/bottom tetraquarks may also exist [17,22,24]. Hence, in this paper we shall investigate tetraquark systems with various spin-parity quantum numbers $J^P = 0^+, 1^+, 2^+$ and $0^-, 1^-$ in the framework of QCD sum rules.

This paper is organized as follows. In Sec. II, we construct the open-flavor charmed/bottom tetraquark interpolating currents and introduce the QCD sum rule formalism. The two-point correlation functions and the spectral densities are calculated for various channels. In Sec. III, we establish stable tetraquark mass sum rules and make reliable predictions for the mass spectra of these tetraquark states. The last section is a brief summary.

II. FORMALISM OF TETRAQUARK SUM RULES

In this section, we will briefly introduce the method of QCD sum rules [47–49] for the tetraquark systems. To begin, we construct the diquark-antidiquark tetraquark operators with one heavy quark and three light quark fields. In the diquark configurations, all models agree that only the color antisymmetric scalar $q_a^T C\gamma_5 q_b$ and axial-vector $q_a^T C\gamma_\mu q_b$ diquark fields are favored to maintain low color electrostatic field energy [50]. To explore the lowest-lying tetraquarks, we use only these two favored S-wave diquarks to compose the color antisymmetric $[\bar{\mathbf{3}}_\mathbf{c}]_{q_1q_2} \otimes [\mathbf{3}_\mathbf{c}]_{\bar{q}_3\bar{Q}}$ tetraquark currents following Refs. [51–54]

$$\begin{aligned}
J_1 &= q_{1a}^T C\gamma_5 q_{2b}(\bar{q}_{3a}\gamma_5 C\bar{Q}_b^T - \bar{q}_{3b}\gamma_5 C\bar{Q}_a^T), \quad J^P = 0^+,\\
J_2 &= q_{1a}^T C\gamma_\mu q_{2b}(\bar{q}_{3a}\gamma^\mu C\bar{Q}_b^T - \bar{q}_{3b}\gamma^\mu C\bar{Q}_a^T), \quad J^P = 0^+,\\
J_{3\mu} &= q_{1a}^T C\gamma_5 q_{2b}(\bar{q}_{3a}\gamma_\mu C\bar{Q}_b^T - \bar{q}_{3b}\gamma_\mu C\bar{Q}_a^T), \quad J^P = 0^-, 1^+,\\
J_{4\mu} &= q_{1a}^T C\gamma_\mu q_{2b}(\bar{q}_{3a}\gamma_5 C\bar{Q}_b^T - \bar{q}_{3b}\gamma_5 C\bar{Q}_a^T), \quad J^P = 0^-, 1^+,\\
J_{5\mu\nu} &= q_{1a}^T C\gamma_\mu q_{2b}(\bar{q}_{3a}\gamma_\nu C\bar{Q}_b^T - \bar{q}_{3b}\gamma_\nu C\bar{Q}_a^T), \quad J^P = 0^+, 1^-,\\
&\quad 2^+(\mathrm{S}); 1^-, 1^+(\mathrm{A}); 0^+(\mathrm{T}),
\end{aligned} \tag{1}$$

in which Q is a heavy quark (c or b) and q_1, q_2, q_3 are light quarks (u, d, s). For the tensor current $J_{5\mu\nu}$, we list its J^P assignments for the traceless symmetric part (S), the antisymmetric part (A) and the trace (T). All these interpolating currents can couple to the tetraquark states that carry the same spin-parity quantum numbers. In this paper, we shall investigate the charm-strange $[sq][\bar{q}\,\bar{c}]$, nonstrange charmed $[qq][\bar{q}\,\bar{c}]$, bottom-strange $[sq][\bar{q}\,\bar{b}]$, and nonstrange bottom $[qq][\bar{q}\,\bar{b}]$ tetraquark systems by using the interpolating currents in Eq. (1), where q is an up or down quark.

We shall study the following two-point correlation functions using the scalar, vector, and tensor currents

$$\Pi(q^2) = i\int d^4x e^{iq\cdot x}\langle 0|T[J(x)J^\dagger(0)]|0\rangle, \tag{2}$$

$$\Pi_{\mu\nu}(q^2) = i\int d^4x e^{iq\cdot x}\langle 0|T[J_\mu(x)J_\nu^\dagger(0)]|0\rangle, \tag{3}$$

$$\Pi_{\mu\nu,\rho\sigma}(q^2) = i\int d^4x e^{iq\cdot x}\langle 0|T[J_{\mu\nu}(x)J_{\rho\sigma}^\dagger(0)]|0\rangle. \tag{4}$$

In general, the two-point functions $\Pi_{\mu\nu}(q^2)$ in Eq. (3) and $\Pi_{\mu\nu,\rho\sigma}(q^2)$ in Eq. (4) contain several different invariant functions referring to pure spin-0, spin-1, or spin-2 hadron states. These invariant functions have distinct tensor structures in $\Pi_{\mu\nu}(q^2)$ and $\Pi_{\mu\nu,\rho\sigma}(q^2)$. For the vector current, it is easy to write the corresponding two-point function as

$$\Pi_{\mu\nu}(q^2) = \eta_{\mu\nu}\Pi_V(q^2) + \frac{q_\mu q_\nu}{q^2}\Pi_S(q^2), \tag{5}$$

where $\eta_{\mu\nu} = q_\mu q_\nu/q^2 - g_{\mu\nu}$ is a projector for the pure spin-1 invariant function $\Pi_V(q^2)$ while $q_\mu q_\nu/q^2$ is a projector for spin-0 invariant function $\Pi_S(q^2)$. To pick out different invariant functions in $\Pi_{\mu\nu,\rho\sigma}(q^2)$ for the tensor current $J_{5\mu\nu}$, we introduce some projectors following Ref. [55]

$$\begin{aligned}
P_{0T} &= \frac{1}{16}g_{\mu\nu}g_{\rho\sigma}, \quad \text{for } J^P = 0^+, \mathrm{T}\\
P_{0S} &= T_{\mu\nu}T_{\rho\sigma}, \quad \text{for } J^P = 0^+, \mathrm{S}\\
P_{0TS} &= \frac{1}{4}(T_{\mu\nu}g_{\rho\sigma} + T_{\rho\sigma}g_{\mu\nu}), \quad \text{for } J^P = 0^+, \mathrm{TS}\\
P_{1A}^N &= T_{\mu\nu,\rho\sigma}^-, \quad \text{for } J^P = 1^-, \mathrm{A}\\
P_{1S}^N &= T_{\mu\nu,\rho\sigma}^+, \quad \text{for } J^P = 1^-, \mathrm{S}\\
P_{1AS}^N &= 2\left(\frac{q_\mu q_\rho}{q^2}\eta_{\nu\sigma} - \frac{q_\nu q_\sigma}{q^2}\eta_{\mu\rho}\right), \quad \text{for } J^P = 1^-, \mathrm{AS}\\
P_{1A}^P &= \eta_{\mu\rho}\eta_{\nu\sigma} - \eta_{\mu\sigma}\eta_{\nu\rho}, \quad \text{for } J^P = 1^+, \mathrm{A}\\
P_{2S}^N &= \left(\eta_{\mu\rho}\eta_{\nu\sigma} + \eta_{\mu\sigma}\eta_{\nu\rho} - \frac{2}{3}\eta_{\mu\nu}\eta_{\rho\sigma}\right), \quad \text{for } J^P = 2^+, \mathrm{S}
\end{aligned} \tag{6}$$

where

$$\begin{aligned}
T_{\mu\nu} &= \frac{q_\mu q_\nu}{q^2} - \frac{1}{4}g_{\mu\nu},\\
T_{\mu\nu,\rho\sigma}^\pm &= \left[\frac{q_\mu q_\rho}{q^2}\eta_{\nu\sigma} \pm (\mu \leftrightarrow \nu)\right] \pm (\rho \leftrightarrow \sigma).
\end{aligned} \tag{7}$$

One notes that in Eq. (6) there are three different projectors for the scalar ($J^P = 0^+$) channel, P_{0T}, P_{0S}, and P_{0TS}, which can be used to pick out different invariant functions induced by the trace part, traceless symmetric part and the cross term respectively from the current $J_{5\mu\nu}$. However, all these three invariant functions couple to the $J^P = 0^+$ channel with different coupling constants. We will discuss all of them in this paper. A similar situation happens for the vector ($J^P = 1^-$) channel in Eq. (6).

As usual, the dispersion relation is used to describe the two-point correlation function at the hadronic level

$$\Pi(q^2)=\frac{(q^2)^N}{\pi}\int_{s<}^{\infty}\frac{\mathrm{Im}\Pi(s)}{s^N(s-q^2-i\epsilon)}ds+\sum_{n=0}^{N-1}b_n(q^2)^n, \quad (8)$$

in which the unknown subtraction constants b_n in the second term can be removed by taking the Borel transform of $\Pi(q^2)$. The imaginary part of the two-point function is usually defined as the spectral function, which can be evaluated at the hadronic level by inserting intermediate hadron states

$$\rho(s)\equiv\frac{\mathrm{Im}\Pi(s)}{\pi}=\sum_n\delta(s-m_n^2)\langle 0|J_\mu|n\rangle\langle n|J_\mu^\dagger|0\rangle \quad (9)$$

$$=f_X^2\delta(s-m_X^2)+\text{continuum}, \quad (10)$$

where the single narrow pole plus continuum parametrization is adopted in the last step. The inserted intermediate states n carry the same quantum numbers as the interpolating current $J_\mu(x)$. The quantity m_X denotes the mass of the lowest lying resonance and f_X is the coupling constant. For the scalar and vector currents, the leptonic coupling constants are defined as

$$\langle 0|J|X\rangle=f_S, \quad (11)$$

$$\langle 0|J_\mu|X\rangle=f_V\epsilon_\mu+f_Sq_\mu, \quad (12)$$

in which ϵ_μ is the polarization vector. For the tensor current, the coupling constants are defined as

$$\begin{aligned}&\langle 0|J_{\mu\nu}|X\rangle\\&=f_{0T}g_{\mu\nu}+f_{0S}q_\mu q_\nu \quad (J^P=0^+)\\&+f_{1S}^-(\epsilon_\mu q_\nu+\epsilon_\nu q_\mu)+f_{1A}^-(\epsilon_\mu q_\nu-\epsilon_\nu q_\mu) \quad (J^P=1^-)\\&+f_{1A}^+\epsilon^{\mu\nu\rho\sigma}\epsilon_\rho q_\sigma \quad (J^P=1^+)\\&+f_{2S}\epsilon_{\mu\nu} \quad (J^P=2^+),\end{aligned} \quad (13)$$

where $\epsilon_{\mu\nu}$ is the polarization tensor and $\epsilon^{\mu\nu\rho\sigma}$ is the completely antisymmetric tensor.

At the quark-gluonic level, the correlation function can be computed by using perturbative QCD augmented with nonperturbative quark and gluon condensates. Comparing the two-point correlation functions at both the hadronic and quark-gluonic levels, one can establish QCD sum rules for hadron parameters like hadron masses, magnetic moments and coupling constants. The technique of Borel transformation is usually adopted to remove the unknown constants in Eq. (8) and suppress the continuum contributions to correlation functions, which results in the Borel sum rules

$$\mathcal{L}_k(s_0,M_B^2)=f_X^2m_X^{2k}e^{-m_X^2/M_B^2}=\int_{M_Q^2}^{s_0}dse^{-s/M_B^2}\rho(s)s^k, \quad (14)$$

in which the lower integral limit $M_Q^2=(m_Q+m_{q_1}+m_{q_2}+m_{q_3})^2$ denotes a physical threshold for the $q_1q_2\bar{q}_3\bar{Q}$ system. The mass of the lowest-lying hadron state is thus obtained as

$$m_X(s_0,M_B^2)=\sqrt{\frac{\mathcal{L}_1(s_0,M_B^2)}{\mathcal{L}_0(s_0,M_B^2)}}, \quad (15)$$

where M_B is the Borel parameter and s_0 is the continuum threshold above which the contributions from the continuum and higher excited states can be approximated well by the QCD spectral function $\rho(s)$.

In this paper, we calculate the correlation functions and spectral densities by considering the perturbative term, quark condensates, gluon condensate, quark-gluon mixed condensates, four-quark condensates and the dimension eight condensates at leading order in α_s. In our evaluation, the strange quark propagator was considered in momentum space. For all interpolating currents in Eq. (1), we collect the expressions of the spectral densities in the Appendix. We use the projectors defined in Eq. (6) to pick out the different invariant functions for the vector and tensor

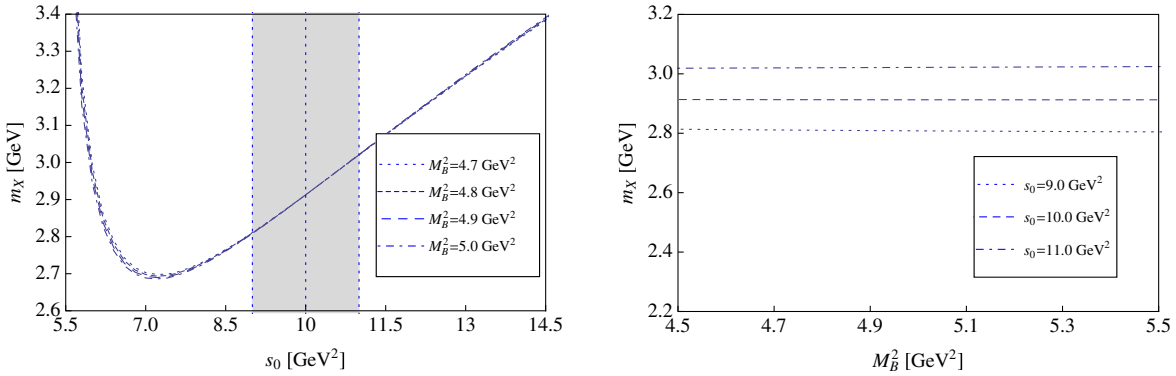

FIG. 1. Variation of the hadron mass m_X with respect to s_0 and M_B^2 for $sq\bar{q}\,\bar{c}$ system with $J^P=0^+$ using the interpolating current $J_2(x)$.

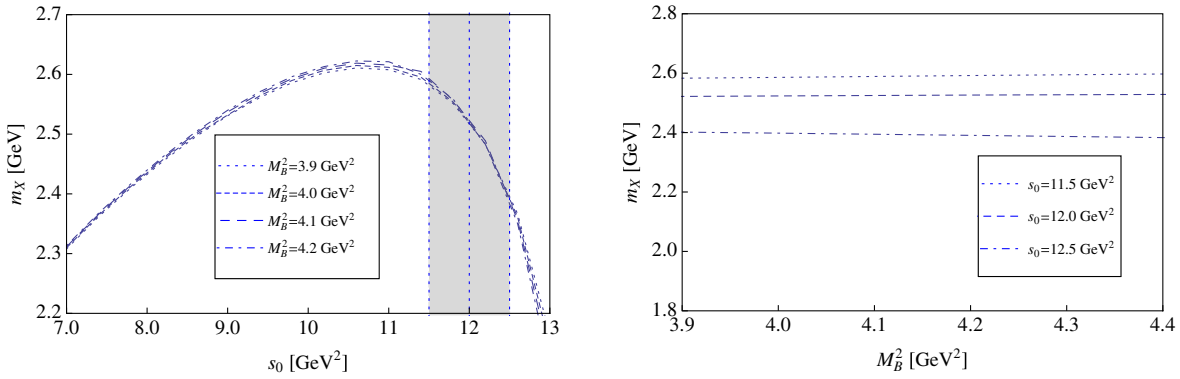

FIG. 2. Variation of the hadron mass m_X with respect to s_0 and M_B^2 for $sq\bar{q}\,\bar{c}$ system with $J^P = 0^+$ (S) using the interpolating current $J_{5\mu\nu}(x)$.

currents. As shown in Eq. (1), the tensor current $J_{5\mu\nu}$ can couple to two different scalar channels ($J^P = 0^+$) as well as two different vector channels ($J^P = 1^-$). We evaluate the invariant functions and spectral densities for all these channels and list them in the Appendix. In addition, one can also find the projectors P_{0TS} (for $J^P = 0^+$ TS) and P_{1AS}^N (for $J^P = 1^-$ AS) in Eq. (6), which can be used to pick out the cross-term invariant functions for the scalar and vector channels respectively. However, we find that the perturbative terms for these two invariant functions are proportional to the light quark mass m_q, which can be neglected in the chiral limit. Such invariant functions cannot provide reliable predictions for hadron properties and thus we will not use them to perform QCD sum rule analyses in this paper.

III. QCD SUM RULE ANALYSIS

In this section, we use the two-point correlation functions obtained above to perform QCD sum rule analyses for the charmed/bottom $su\bar{d}\,\bar{Q}$ and $ud\bar{d}\,\bar{Q}$ tetraquark systems, in which the following parameter values for the quark masses and QCD condensates are adopted [1,48,56,57]

$$\begin{aligned} m_u &= m_d = 0, \\ m_s(2\ \text{GeV}) &= (96^{+8}_{-4})\ \text{MeV}, \\ m_c(m_c) &= \bar{m}_c = (1.27 \pm 0.03)\ \text{GeV}, \\ m_b(m_b) &= \bar{m}_b = (4.18^{+0.04}_{-0.03})\ \text{GeV}, \\ \langle \bar{q}q \rangle &= -(0.24 \pm 0.01)^3\ \text{GeV}^3, \\ \langle \bar{s}s \rangle &= (0.8 \pm 0.1)\langle \bar{q}q \rangle, \\ \langle \bar{q} g_s \sigma \cdot G q \rangle &= -M_0^2 \langle \bar{q}q \rangle, \\ \langle \bar{s} g_s \sigma \cdot G s \rangle &= -M_0^2 \langle \bar{s}s \rangle, \\ M_0^2 &= (0.8 \pm 0.2)\ \text{GeV}^2, \\ \langle g_s^2 GG \rangle &= (0.48 \pm 0.14)\ \text{GeV}^4, \end{aligned} \tag{16}$$

where we use the "running masses" for the heavy quarks in the $\overline{\text{MS}}$ scheme. We use the chiral limit in our analysis in which the up and down quark masses $m_u = m_d = m_q = 0$.

As shown in Eq. (15), the extracted hadron mass is a function of the Borel parameter M_B and the continuum threshold s_0. To obtain a reliable mass sum rule analysis, one should choose suitable working ranges for these two free parameters. We determine the lower bound on the

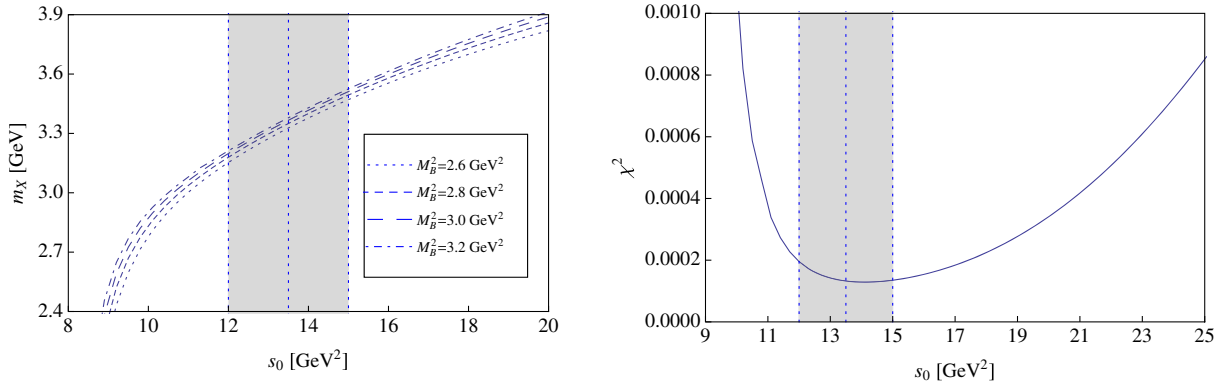

FIG. 3. Left panel: hadron mass m_X as a function of s_0 for the $sq\bar{q}\,\bar{c}$ system using the traceless antisymmetric part of $J_{5\mu\nu}(x)$ with $J^P = 1^-$(A). Right panel: the quantity χ^2 as the function of the continuum threshold s_0.

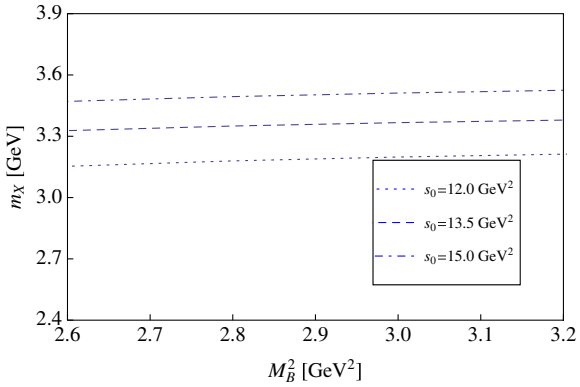

FIG. 4. Mass prediction for the $sq\bar{q}\,\bar{c}$ system with $J^P = 1^-(\mathrm{A})$.

Borel parameter by requiring the perturbative term contribution be larger than three times of the dominant nonperturbative terms. The study of the pole contribution can yield the upper bound on M_B. For the continuum threshold s_0, we will choose a reasonable value to minimize the dependance of the extracted hadron mass with respect to M_B. In the following, we will use the $sq\bar{q}\bar{c}$ systems as examples to discuss the detail of the numerical analyses for all channels, which can be classified into three types:

(A) This type can provide stable mass sum rules and give reliable mass predictions. We use the interpolating current $J_2(x)$ with $J^P = 0^+$ as an example to perform the numerical analysis. As shown in the left panel of Fig. 1, we show the variation of m_X with respect to the continuum threshold s_0 for different value of the Borel mass M_B^2. We find that there are some minimum points around which m_X is stable at $s_0 = 7.0$ GeV^2. For larger continuum threshold after these points, the hadron mass will increase gradually with s_0 and the curves with different values of M_B^2 intersect at $s_0 = 10.0$ GeV^2. Thus we can determine the optimal working range for the continuum threshold with a reasonable 10% uncertainty to be $9.0 \leq s_0 \leq 11.0$ GeV^2 (shaded region in the left panel of Fig. 1), in which the M_B dependance of m_X will be very weak. Accordingly, we can also obtain the Borel window as $4.7 \leq M_B^2 \leq 5.0$ GeV^2 by studying the operator product expansion (OPE) convergence and pole contribution. We show the Borel curves in the right panel of Fig. 1 for the hadron mass m_X. One notes that the sum rules are very stable in the Borel window and the extracted hadron mass increases with respect to s_0. Using the central value $s_0 = 10.0$ GeV^2, we can extract the hadron mass for the $J^P = 0^+$ $sq\bar{q}\bar{c}$ tetraquark state

TABLE I. Mass spectrum for the charm-strange $sq\bar{q}\,\bar{c}$ tetraquark states.

J^{PC}	Currents	s_0(GeV^2)	Borel window (GeV^2)	$m_{X^{cs}}$(GeV)	Type
0^+	J_1	7.5 ± 0.5	3.3–3.6	2.55 ± 0.10	A
	J_2	10.0 ± 0.5	4.7–5.0	2.91 ± 0.14	A
	$J_{5\mu\nu}$(T)	10.0 ± 0.5	2.2–3.1	2.88 ± 0.15	A
	$J_{5\mu\nu}$(S)	12.0 ± 0.5	3.9–4.2	2.53 ± 0.13	B
1^+	$J_{3\mu}$	7.5 ± 0.5	5–3.8	2.55 ± 0.12	A
	$J_{4\mu}$	9.5 ± 0.5	3.2–3.9	2.81 ± 0.13	A
	$J_{5\mu\nu}$(A)	9.5 ± 0.5	3.5–3.8	2.83 ± 0.13	A
2^+	$J_{5\mu\nu}$(S)	10.0 ± 0.5	3.4–4.0	2.91 ± 0.13	A
0^-	$J_{3\mu}$	7.5 ± 0.5	4.0–4.3	2.31 ± 0.09	A
	$J_{4\mu}$	12.0 ± 0.5	3.2–4.1	3.30 ± 0.16	A
1^-	$J_{5\mu\nu}$(A)	13.5 ± 1.0	2.6–3.4	3.35 ± 0.16	C
	$J_{5\mu\nu}$(S)	15.5 ± 1.0	3.2–3.9	3.55 ± 0.18	C

TABLE II. Mass spectrum for the nonstrange charmed $qq\bar{q}\,\bar{c}$ tetraquark states.

J^{PC}	Currents	s_0(GeV^2)	Borel window (GeV^2)	$m_{X^{cq}}$(GeV)	Type
0^+	J_1	9.5 ± 0.5	3.1–4.0	2.82 ± 0.12	A
	J_2	10.0 ± 0.5	4.4–5.0	2.91 ± 0.13	A
	$J_{5\mu\nu}$(T)	10.5 ± 0.5	2.1–2.6	2.93 ± 0.13	A
	$J_{5\mu\nu}$(S)	8.5 ± 0.5	2.4–3.3	2.23 ± 0.12	B
1^+	$J_{3\mu}$	9.5 ± 0.5	3.3–3.9	2.83 ± 0.12	A
	$J_{4\mu}$	10.0 ± 0.5	3.0–4.2	2.88 ± 0.12	A
	$J_{5\mu\nu}$(A)	9.5 ± 0.5	3.3–3.9	2.82 ± 0.12	A
2^+	$J_{5\mu\nu}$(S)	10.0 ± 0.5	3.2–4.1	2.90 ± 0.15	A
0^-	$J_{3\mu}$	6.5 ± 0.5	4.1–4.4	2.21 ± 0.06	A
	$J_{4\mu}$	13.0 ± 0.5	3.4–4.0	3.29 ± 0.15	C
1^-	$J_{5\mu\nu}$(A)	13.5 ± 1.0	2.7–3.3	3.29 ± 0.16	C
	$J_{5\mu\nu}$(S)	15.5 ± 1.0	3.3–4.0	3.52 ± 0.17	C

TABLE III. Mass spectrum for the bottom-strange $sq\bar{q}\,\bar{b}$ tetraquark states.

J^{PC}	Currents	s_0(GeV^2)	Borel window (GeV^2)	$m_{X^{bs}}$(GeV)	Type
0^+	J_1	34.0 ± 2.0	6.0–6.3	5.59 ± 0.18	A
	J_2	37.0 ± 2.0	8.4–8.7	5.83 ± 0.21	A
	$J_{5\mu\nu}$(T)	41.0 ± 2.0	4.3–5.3	6.02 ± 0.21	A
	$J_{5\mu\nu}$(S)	61.0 ± 2.0	6.1–7.3	7.32 ± 0.21	A
1^+	$J_{3\mu}$	34.0 ± 2.0	6.3–6.6	5.59 ± 0.19	A
	$J_{4\mu}$	38.0 ± 2.0	6.0–7.3	5.86 ± 0.20	A
	$J_{5\mu\nu}$(A)	38.0 ± 2.0	6.3–7.4	5.88 ± 0.18	A
2^+	$J_{5\mu\nu}$(S)	40.0 ± 2.0	6.2–8.0	6.01 ± 0.22	A
0^-	$J_{3\mu}$	38.0 ± 2.0	6.6–6.9	5.62 ± 0.24	A
	$J_{4\mu}$	43.0 ± 2.0	5.5–6.7	6.32 ± 0.18	A
1^-	$J_{5\mu\nu}$(A)	43.0 ± 2.0	4.4–5.0	6.19 ± 0.25	C
	$J_{5\mu\nu}$(S)	44.0 ± 2.0	4.8–5.5	6.22 ± 0.27	C

TABLE IV. Mass spectrum for the nonstrange bottom $qq\bar{q}\,\bar{b}$ tetraquark states.

J^{PC}	Currents	$s_0(\mathrm{GeV}^2)$	Borel window (GeV^2)	$m_{X^{bq}}(\mathrm{GeV})$	Type
0^+	J_1	38.0 ± 2.0	5.8–7.4	5.86 ± 0.20	A
	J_2	37.0 ± 2.0	8.0–8.3	5.83 ± 0.20	A
	$J_{5\mu\nu}(\mathrm{T})$	41.0 ± 2.0	4.3–5.3	6.02 ± 0.21	A
	$J_{5\mu\nu}(\mathrm{S})$	52.0 ± 2.0	5.1–5.6	6.74 ± 0.24	C
1^+	$J_{3\mu}$	38.0 ± 2.0	6.1–7.4	5.87 ± 0.21	A
	$J_{4\mu}$	40.0 ± 2.0	5.8–6.7	5.98 ± 0.21	A
	$J_{5\mu\nu}(\mathrm{A})$	38.0 ± 2.0	6.1–7.4	5.86 ± 0.21	A
2^+	$J_{5\mu\nu}(\mathrm{S})$	40.0 ± 2.0	6.0–6.7	5.99 ± 0.21	A
0^-	$J_{3\mu}$	37.0 ± 2.0	6.8–7.1	5.51 ± 0.25	A
	$J_{4\mu}$	44.0 ± 2.0	5.6–6.0	6.23 ± 0.24	C
1^-	$J_{5\mu\nu}(\mathrm{A})$	40.0 ± 2.0	4.1–4.7	5.88 ± 0.27	C
	$J_{5\mu\nu}(\mathrm{S})$	41.0 ± 2.0	4.5–5.0	5.94 ± 0.27	C

$$m_{X^{cs}_{0^+,2}} = (2.91 \pm 0.11 \pm 0.07 \pm 0.04 \pm 0.01)\ \mathrm{GeV}, \tag{17}$$

in which the errors come from the uncertainties in the threshold values s_0, M_0^2, various QCD condensates and the charm quark mass, respectively.

(B) In this type we consider the traceless symmetric part of the interpolating current $J_{5\mu\nu}(x)$ in the scalar channel with $J^P = 0^+$ (S). In the left panel of Fig. 2, we show the variation of the m_X with respect to the continuum threshold s_0 in the Borel window $3.9 \leq M_B^2 \leq 4.2\ \mathrm{GeV}^2$. We find that the behaviour of these s_0-dependance curves is very different from those in type A as shown in Fig. 1. Instead of minimum points for type A, the s_0-dependance curves in type B have maximum points and then the extracted hadron mass decreases gradually with respect to s_0. However, we are still able to find the optimal values for the continuum threshold $11.5 \leq s_0 \leq 12.5\ \mathrm{GeV}^2$ to minimize the dependance of m_X on the Borel mass M_B^2. In this working range, we plot the stable Borel curves in the right panel of Fig. 2 in the above Borel window, from which the extracted hadron mass decreases with respect to s_0. We finally obtain

$$m_{X^{cs}_{0^+,s}} = (2.52 \pm 0.10 \pm 0.11 \pm 0.06 \pm 0.05)\ \mathrm{GeV}, \tag{18}$$

in which the errors come from the uncertainties in the threshold values s_0, M_0^2, various QCD condensates and the charm quark mass, respectively.

TABLE V. Possible S-wave decay modes for the open-flavor charmed/bottom tetraquark states where "–" denotes that the predicted tetraquark masses are below all allowed S-wave two-body hadronic decay thresholds.

$I(J^P)$	$sq\bar{q}\,\bar{b}$	$sq\bar{q}\,\bar{c}$	$I(J^P)$	$qq\bar{q}\,\bar{b}$	$qq\bar{q}\,\bar{c}$
$0(0^+)$	$B_s^0\eta/\eta'$, $B_s^*\omega/\phi$, $B^*K^*(892)$, $B_{s1}(5830)^0 h_1(1170)/f_1(1285)$, $B_1(5721)^0 K_1(1270)$, BK	$D_s\eta/\eta'$, $D_s^*\omega$, DK	$\frac{1}{2}(0^+)$	$B\eta/\eta'$, $B^*\omega/\phi$, $B\pi$, $B^*\rho$	$D\pi/\eta/\eta'$, $D^*\omega/\rho$
$1(0^+)$	$B_s^0\pi$, BK, $B_s^*\rho$, $B^*K^*(892)$, $B_{s1}(5830)^0 b_1(1235)/a_1(1260)$, $B_1(5721)^0 K_1(1270)$	$D_s\pi$, $D_s^*\rho$, DK	$\frac{3}{2}(0^+)$	$B\pi$, $B^*\rho$	$D\pi$, $D^*\rho$
$0(1^+)$	–	–	$\frac{1}{2}(1^+)$	$B^*\pi$, $B\omega$	$D^*\pi$, $D\omega/\rho$
$1(1^+)$	$B_s^*\pi$	$D_s^*\pi$	$\frac{3}{2}(1^+)$	$B^*\pi$, $B\rho$	$D^*\pi$, $D\rho$
$0(2^+)$	–	$D_s^*\omega$	$\frac{1}{2}(2^+)$	–	$D^*(2007)^0\omega/\rho$
$1(2^+)$	–	$D_s^*\rho$	$\frac{3}{2}(2^+)$	–	$D^*(2007)^0\rho$
$0(0^-)$	$B_s^0\sigma$	$D_s\sigma/f_0(980)$	$\frac{1}{2}(0^-)$	$B\sigma$	$D\sigma/a_0/f_0$, $D_0^*(2400)\pi$
$1(0^-)$	–	$D_s a_0(980)$, $D_{s0}^*(2317)\pi$	$\frac{3}{2}(0^-)$	–	$Da_0(980)$, $D_0^*(2400)\pi$
$0(1^-)$	–	$D_s h_1(1170)/f_1(1285)$, $D_s^*\sigma/f_0(980)$, $D_{s0}^*(2317)\omega$, $D_{s1}(2536)\omega$, $D_s^* h_1(1170)$	$\frac{1}{2}(1^-)$	$B_1(5721)^0\pi$	$Dh_1/f_1/a_1/b_1$, $D_0^*\omega/\rho$, $D^*\sigma/f_0/a_0$, $D^* h_1/b_1$, $D_1(2420)^0\omega/\rho/\pi$
$1(1^-)$	$B_{s1}(5830)^0\pi$	$D_s b_1(1235)/a_1(1260)$, $D_{s1}(2460)\pi$, $D_{s0}^*(2317)\rho$, $D_s^* a_0(980)$, $D_{s1}(2536)\rho$	$\frac{3}{2}(1^-)$	$B_1(5721)^0\pi$	$D^* a_0$, Da_1/b_1, $D_0^*\rho$, $D_0^*(2400)\pi/\rho$, $D^*(2007)^0 b_1$

TABLE VI. Possible P-wave decay modes for the open-flavor charmed/bottom tetraquark states.

$I(J^P)$	$sq\bar{q}\,\bar{b}$	$sq\bar{q}\,\bar{c}$	$I(J^P)$	$qq\bar{q}\,\bar{b}$	$qq\bar{q}\,\bar{c}$
$0(0^+)$	$B_s^0h_1/f_1$, $B_s^*\sigma/f_0$, $BK_1(1270)$, $B_{s1}(5830)^0\omega/\phi$, $B_s^*h_1/f_1$, $B_1(5721)^0K^*(892)$, B^*K_1/K_0^*	$D_s^*\sigma$	$\frac{1}{2}(0^+)$	$Bh_1/f_1/b_1/a_1$, $B^*\sigma/f_0/h_1/b_1/a_1$, $B_1(5721)^0\pi/\rho/\omega/\phi$	$D_1(2420)\pi$, $D^*\sigma$,
$1(0^+)$	$B_{s1}(5830)^0\pi/\rho$, $B_s^*a_0$, BK_1, $B_s^0b_1/a_1$, $B_s^*a_0/b_1/a_1$, $B_1(5721)^0K^*(892)$, B^*K_1/K_0^*	$D_{s1}(2460)\pi$	$\frac{3}{2}(0^+)$	Bb_1/a_1, $B^*a_0/b_1/a_1$, $B_1(5721)^0\pi/\rho$	$D_1(2420)\pi$,
$0(1^+)$	$B_s^0/B_s^*\sigma$	$D_s/D_s^*\sigma$	$\frac{1}{2}(1^+)$	$B/B^*\sigma$, $B_1(5721)^0\pi$	$D_1(2420)\pi$, $D/D^*\sigma$
$1(1^+)$	$B_{s1}(5830)^0\pi$	$D_{s1}(2460)\pi$	$\frac{3}{2}(1^+)$	$B_1(5721)^0\pi$	$D_1(2420)\pi$
$0(2^+)$	$B_s^*\sigma$	$D_s^*\sigma$	$\frac{1}{2}(2^+)$	$B^*\sigma$, $B_1(5721)^0\pi$	$D_1(2420)\pi$, $D^*\sigma$
$1(2^+)$	$B_{s1}(5830)^0\pi$	$D_{s1}(2460)\pi$	$\frac{3}{2}(2^+)$	$B_1(5721)^0\pi$	$D_1(2420)\pi$
$0(0^-)$	$B_s^0\omega$, $B_s^*\eta/\eta'/\omega$, B^*K, B/B^*K^*	$D_s\omega$, $D_s^*\eta/\eta'\omega$, $D_{s1}\sigma$, D^*K, D/D^*K^*	$\frac{1}{2}(0^-)$	$B^*\pi/\eta/\eta'$, $B\rho/\omega$, $B^*\rho/\omega$	$D\rho/\omega/\phi$, $D^*\pi/\eta/\eta'$, $D^*\rho/\omega/\phi$, $D_1(2420)\sigma$
$1(0^-)$	$B_s^0\rho$, $B_s^*\pi/\rho$, B^*K, B/B^*K^*	$D_s\rho$, $D_s^*\pi/\rho$, D^*K, D/D^*K^*	$\frac{3}{2}(0^-)$	$B^*\pi/\rho$, $B\rho$	$D/D^*\rho$, $D^*\pi$
$0(1^-)$	$B_s^0\omega$, BK,	$D_s\eta/\eta'/\omega$, $D_s^*\omega/\eta/\eta'$, $D_{s1}\sigma$, D/D^*K, D/D^*K^*	$\frac{1}{2}(1^-)$	$B/B^*\pi$	$D\pi/\eta/\eta'/\rho/\omega/\phi$, $D^*\pi/\eta/\eta'/\rho/\omega/\phi$
$1(1^-)$	$B_s^*\pi$, $B_s^0\rho/\pi$, BK	$D_s\pi/\rho$, $D_s^*\pi/\rho$, D/D^*K, D/D^*K^*	$\frac{3}{2}(1^-)$	$B/B^*\pi$	$D\pi/\rho$, $D^*\pi/\rho$

(C) In the third type we study the traceless antisymmetric part of the interpolating current $J_{5\mu\nu}(x)$ in the vector channel with $J^P = 1^-$ (A). We first study the variation of the hadron mass with s_0 in its Borel window $2.6 \leq M_B^2 \leq 3.2$ GeV^2. As shown in the left panel of Fig. 3, the behavior is totally different from those in types A and B. The extracted hadron mass m_X increases monotonically with s_0 without any minimum or maximum point and the curves with different value of M_B^2 do not intersect anywhere. It seems that the mass sum rules are unstable in this situation. To explore the further behavior of s_0-dependance, we define the following hadron mass

$$\bar{m}_X(s_0) = \sum_{i=1}^{N} \frac{m_X(s_0, M_{B,i}^2)}{N}, \tag{19}$$

in which the $M_{B,i}^2 (i = 1, 2, \ldots, N)$ represent N definite values for the Borel parameter M_B^2 in the Borel window $2.6 \leq M_B^2 \leq 3.2$ GeV^2. The $\bar{m}_X(s_0)$ is defined as an averaged hadron mass for some definite value M_B^2. Using this average hadron mass, we can define the following quantity

$$\chi^2(s_0) = \sum_{i=1}^{N} \left[\frac{m_X(s_0, M_{B,i}^2)}{\bar{m}_X(s_0)} - 1\right]^2. \tag{20}$$

According to the above definition, the optimal choice for the continuum threshold s_0 in the QCD sum rule analysis can be obtained by minimizing the quantity $\chi^2(s_0)$, which is only the function of s_0. We show this relation in the right panel of Fig. 3, from which there is a minimum point around $s_0 = 13.5$ GeV^2. It is clearly that the M_B^2-dependance for the extracted hadron mass is the weakest at this point. We can thus determine the working range for the continuum threshold to be $12.0 \leq s_0 \leq 15.0$ GeV^2 in our analysis, as shown in the left panel of Fig. 3. In this area, we show m_X as a function of the Borel parameter M_B^2 in Fig. 4 and predict the hadron mass at the central values $s_0 = 13.5$ GeV^2, $M_B^2 = 2.9$ GeV^2 to be

$$m_{X^{cs}_{1^-A}} = (3.35 \pm 0.14 \pm 0.07 \pm 0.04 \pm 0.01)\ \text{GeV}, \tag{21}$$

in which the errors come from the uncertainties in the threshold values s_0, M_0^2, various QCD condensates and the charm quark mass, respectively.

For all interpolating currents in Eq. (1), we perform similar numerical analyses and collect the extracted hadron masses for the $sq\bar{q}\,\bar{c}$ tetraquark states in Table I, together with the Borel windows and the working ranges for s_0. We show the three types introduced above in the last column. The error sources for the hadron masses include the uncertainties of the heavy quark masses, the QCD condensates, M_0^2, and the uncertainty of the continuum threshold s_0. As shown in Eqs. (17), (18), and (21), the uncertainty

in s_0 is the dominant error source of the hadron mass while that of M_0^2 parametrizing the mixed condensate is also important. However, we list only the total errors in Table I with error analyses to summarize the results. In Table I, we find that the extracted masses for the scalar $sq\bar{q}\bar{c}$ charmed tetraquarks with $J^P = 0^+$ to be almost degenerate around 2.54 GeV from the currents $J_1(x)$ and $J_{5\mu\nu}(x)(\mathrm{S})$, while 2.90 GeV from the currents $J_2(x)$ and $J_{5\mu\nu}(x)(\mathrm{T})$. These values for the scalar charmed tetraquarks are higher than the mass of the charm-strange $D_{s0}^*(2317)$ meson. In addition, we obtain the hadron mass $m_{X_{cs}} = (2.55 \pm 0.12)$ GeV for the axial-vector $sq\bar{q}\bar{c}$ tetraquark using the current $J_{3\mu}(x)$ with $J^P = 1^+$. This result is not far from the mass of the narrow charm-strange $D_{s1}(2460)$ meson within the error.

Replacing the strange quark in $sq\bar{q}\bar{c}$ systems to be a down quark, we can study the nonstrange charmed tetraquark systems $qq\bar{q}\bar{c}$ in similar way as the above analyses. The OPE series are a bit different by changing the condensates $\langle\bar{s}s\rangle$, $\langle\bar{s}Gs\rangle$ into $\langle\bar{q}q\rangle$, $\langle\bar{q}Gq\rangle$ respectively and neglecting the m_q proportional terms in the chiral limit. The numerical results for these systems are then obtained and collected in Table II. Similarly, we can easily study the strange and nonstrange bottom tetraquark systems $sq\bar{q}\bar{b}$ and $qq\bar{q}\bar{b}$ in the heavy quark symmetry. After performing the QCD sum rule analyses, we collect the numerical results for the $sq\bar{q}\bar{b}$ and $qq\bar{q}\bar{b}$ systems in Tables III and IV, respectively. In Table III, the masses for the bottom-strange $sq\bar{q}\bar{b}$ tetraquarks extracted from the interpolating currents $J_1(x)$ and $J_{3\mu}(x)$ were previously obtained in Ref. [12], which were used to explain the newly reported $X(5568)$ structure.

Except for the scalar and axial-vector states, we also investigate the other channels with $J^P = 0^-, 1^-, 2^+$ and collect the results in Tables I–IV.

IV. DECAY PROPERTIES OF THE OPEN-FLAVOR CHARMED/BOTTOM TETRAQUARKS

Using the mass spectra obtained above, we can study the possible decay patterns of the $sq\bar{q}\bar{c}$, $qq\bar{q}\bar{c}$, $sq\bar{q}\bar{b}$, $qq\bar{q}\bar{b}$ tetraquark states in various channels. These open-flavor charmed/bottom tetraquarks will decay easily through the fall-apart mechanism so long as the kinematics allows. We study both the S-wave and P-wave two-body hadronic decays by considering the conservation of the angular momentum, parity and isospin in Tables V and VI.

In Table V, we list the possible S-wave two-body hadronic decay modes for the $sq\bar{q}\bar{c}$, $qq\bar{q}\bar{c}$, $sq\bar{q}\bar{b}$, $qq\bar{q}\bar{b}$ tetraquark states with various quantum numbers. We consider isospin-0/1 for $sq\bar{q}\bar{c}$, $sq\bar{q}\bar{b}$ states and isospin-$\frac{1}{2}/\frac{3}{2}$ for $qq\bar{q}\bar{c}$, $qq\bar{q}\bar{b}$ states, respectively. In the chiral limit, these tetraquarks in the same isospin multiplet are predicted to be degenerate since we do not differentiate between the up and down quarks. For the charmed/bottom-strange $sq\bar{q}\bar{c}$ and $sq\bar{q}\bar{b}$ states, their decay patterns are very different for the isospin-scalar and isospin-vector channels except some one D/B meson plus one K meson decay modes. Such decays are allowed by the isospin symmetry for both channels. However, the situation is different for the nonstrange $qq\bar{q}\bar{c}$ and $qq\bar{q}\bar{b}$ tetraquarks. In Table V, one notes that all possible decay modes for the isospin-$\frac{3}{2}$ states are allowed for the corresponding isospin-$\frac{1}{2}$ ones.

As shown in Table V, there is no allowed S-wave decay modes for the tensor $sq\bar{q}\bar{b}$ states. This is because the predicted hadron mass for these tetraquarks in Table III is lower than any possible S-wave two-body hadronic decay threshold. There also exist some other tetraquark states below the S-wave decay thresholds, which are denoted by "–" in Table V. However, it is shown that the P-wave decays are allowed for these states, as shown in Table VI. This means that the P-wave decay modes are dominant for these tetraquark states and thus they are much narrower than other states. These tetraquark states will be prime candidates for observation.

V. CONCLUSIONS AND DISCUSSION

In this paper, we have studied the open-flavor charmed/bottom $sq\bar{q}\bar{c}$, $qq\bar{q}\bar{c}$, $sq\bar{q}\bar{b}$, $qq\bar{q}\bar{b}$ tetraquark states with the spin-parity quantum numbers $J^P = 0^+, 1^+, 2^+$ and $0^-, 1^-$. In the diquark configurations, we use only the color-antisymmetric scalar and axial-vector diquarks to compose the color-antisymmetric $[\bar{\mathbf{3}}_\mathbf{c}]_{\mathrm{diquark}} \otimes [\mathbf{3}_\mathbf{c}]_{\mathrm{antidiquark}}$ tetraquark interpolating currents. Finally, we obtain five tetraquark currents in Eq. (1) with various spin-parity quantum numbers.

After performing the numerical analyses, we obtained the hadron masses for the open-flavor charmed/bottom $sq\bar{q}\bar{c}$, $qq\bar{q}\bar{c}$, $sq\bar{q}\bar{b}$, $qq\bar{q}\bar{b}$ tetraquark states. For the charm-strange $sq\bar{q}\,\bar{c}$ systems, we extract the hadron mass $m_{X_{cs}} = (2.55 \pm 0.12)$ GeV using the interpolating current $J_{3\mu}(x)$ with $J^P = 1^+$, which is not far from the mass of the $D_{s1}(2460)$ meson within the error. In the scalar channel, however, the results for the $sq\bar{q}\bar{c}$ systems disfavor the tetraquark explanation of the charm-strange $D_{s0}^*(2317)$ meson.

Our results indicate that many other charmed/bottom tetraquarks may exist, and we have evaluated their masses. The tetraquarks $[su][\bar{d}\,\bar{c}]$, $\frac{[su][\bar{u}\,\bar{c}]+[sd][\bar{d}\,\bar{c}]}{\sqrt{2}}$, and $[sd][\bar{u}\,\bar{c}]$ can form an isotriplet. Since we do not differentiate the up and down quarks in the OPE series, these tetraquark states in the same isospin multiplet have the same extracted hadron masses in our analyses. In other words, the mass spectra in Tables I–IV contain all open-flavor charmed/bottom tetraquarks. Among these states, the exotic doubly-charged tetraquarks, such as $[sd][\bar{u}\,\bar{c}] \to D_s^{(*)-}\pi^-$, is especially interesting, and have not been observed so far. Our results for their mass spectra can be useful for their searches in

future experiments at facilities such as BESIII, BelleII, PANDA, LHCb, CMS, etc.

ACKNOWLEDGMENTS

This project is supported by the Natural Sciences and Engineering Research Council of Canada (NSERC) and the National Natural Science Foundation of China under Grants No. 11475015, No. 11375024, No. 11222547, No. 11175073, No. 11575008, and No. 11621131001; the 973 program; the Ministry of Education of China (SRFDP under Grant No. 20120211110002 and the Fundamental Research Funds for the Central Universities); the National Program for Support of Top-notch Youth Professionals.

APPENDIX: SPECTRAL DENSITIES

In this appendix, we collect the spectral densities for all interpolating currents defined in Eq. (1). To calculate these spectral densities, we use the momentum space propagators for the heavy quarks (bottom and charm) and strange quark while coordinate space propagators for the light quarks

$$
\begin{aligned}
iS_Q^{ab} &= \frac{i\delta^{ab}}{\hat{p}-m_Q} + \frac{i}{4}g_s\frac{\lambda_{ab}^n}{2}G_{\mu\nu}^n\frac{\sigma^{\mu\nu}(\hat{p}+m_Q)+(\hat{p}+m_Q)\sigma^{\mu\nu}}{(p^2-m_Q^2)^2} + \frac{i\delta^{ab}}{12}\langle g_s^2GG\rangle m_Q\frac{p^2+m_Q\hat{p}}{(p^2-m_Q^2)^4},\\
iS_q^{ab} &= \frac{i\delta^{ab}}{2\pi^2x^4}\hat{x} + \frac{i}{32\pi^2}\frac{\lambda_{ab}^n}{2}g_sG_{\mu\nu}^n\frac{1}{x^2}(\sigma^{\mu\nu}\hat{x}+\hat{x}\sigma^{\mu\nu}) - \frac{\delta^{ab}}{12}\langle\bar{q}q\rangle + \frac{\delta^{ab}x^2}{192}\langle g_s\bar{q}\sigma\cdot Gq\rangle - \frac{m_q\delta^{ab}}{4\pi^2x^2} + \frac{i\delta^{ab}m_q\langle\bar{q}q\rangle}{48}\hat{x},
\end{aligned}
\tag{A1}
$$

where $\hat{x}=\gamma_\mu x^\mu$, $\hat{p}=\gamma_\mu p^\mu$. The nonperturbative terms correlated to $\langle\bar{s}s\rangle$ and $\langle\bar{s}g_s\sigma\cdot Gs\rangle$ are also calculated by considering the various strange quark condensates. We will use the projectors defined in Eq. (6) to pick out the different invariant functions and also the spectral densities for the vector and tensor currents. Up to dimension eight, the spectral density can be written as

$$
\rho(s)=\rho^{\text{pert}}(s)+\rho^{\langle\bar{q}q\rangle}(s)+\rho^{\langle GG\rangle}(s)+\rho^{\langle\bar{q}Gq\rangle}(s)+\rho^{\langle\bar{q}q\rangle^2}(s)+\rho^{\langle\bar{q}q\rangle\langle\bar{q}Gq\rangle}. \tag{A2}
$$

(i) For the current $J_1(x)$ with $J^P=0^+$

$$
\begin{aligned}
\rho_1^{\text{pert}}(s) &= \frac{1}{512\pi^6}\int_{\alpha_{\min}}^{\alpha_{\max}}d\alpha\int_{\beta_{\min}}^{\beta_{\max}}d\beta\frac{(1-\alpha-\beta)^2(\alpha m_s^2+\beta m_Q^2-\alpha\beta s)^3(\alpha m_s^2+\beta m_Q^2-3\alpha\beta s)}{\alpha^3\beta^3},\\
\rho_1^{\langle\bar{q}q\rangle}(s) &= -\frac{\langle\bar{q}q\rangle}{16\pi^4}\int_{\alpha_{\min}}^{\alpha_{\max}}d\alpha\int_{\beta_{\min}}^{\beta_{\max}}d\beta\left(\frac{m_Q}{\alpha}+\frac{m_s}{\beta}\right)\frac{(1-\alpha-\beta)(\alpha m_s^2+\beta m_Q^2-\alpha\beta s)(\alpha m_s^2+\beta m_Q^2-2\alpha\beta s)}{\alpha\beta},\\
\rho_1^{\langle\bar{s}s\rangle}(s) &= \frac{m_s\langle\bar{s}s\rangle(s-m_Q^2)(s^2-5m_Q^2s-2m_Q^4)}{384\pi^4s} - \frac{m_Q^4m_s\langle\bar{s}s\rangle\log[m_Q^2/s]}{64\pi^4},\\
\rho_1^{\langle GG\rangle}(s) &= \frac{\langle g_s^2GG\rangle}{1024\pi^6}\int_{\alpha_{\min}}^{\alpha_{\max}}d\alpha\int_{\beta_{\min}}^{\beta_{\max}}d\beta\left[\left(\frac{m_Q^2}{\alpha^3}+\frac{m_s^2}{\beta^3}\right)\frac{(1-\alpha-\beta)^2(2\alpha m_s^2+2\beta m_Q^2-3\alpha\beta s)}{3}\right.\\
&\quad\left.+\left(\frac{1}{\alpha}+\frac{1}{\beta}\right)\frac{(1-\alpha-\beta)(\alpha m_s^2+\beta m_Q^2-\alpha\beta s)(\alpha m_s^2+\beta m_Q^2-2\alpha\beta s)}{\alpha\beta}\right],\\
\rho_1^{\langle\bar{q}Gq\rangle}(s) &= \frac{\langle\bar{q}g_s\sigma\cdot Gq\rangle}{64\pi^4}\int_{\alpha_{\min}}^{\alpha_{\max}}d\alpha\int_{\beta_{\min}}^{\beta_{\max}}d\beta\left[\left(\frac{m_Q}{\alpha}+\frac{m_s}{\beta}\right)\right.\\
&\quad\left.-\left(\frac{m_Q}{\alpha^2}+\frac{m_s}{\beta^2}\right)(1-\alpha-\beta)\right](2\alpha m_s^2+2\beta m_Q^2-3\alpha\beta s),\\
\rho_1^{\langle\bar{q}q\rangle^2}(s) &= \frac{m_Qm_s\langle\bar{q}q\rangle^2}{12\pi^2}\sqrt{\left(1-\frac{m_Q^2-m_s^2}{s}\right)^2-\frac{4m_s^2}{s}} + \frac{\langle\bar{q}q\rangle\langle\bar{s}s\rangle(s-m_Q^2)(s-m_Qm_s-m_Q^2)}{24\pi^2s},\\
\rho_1^{\langle\bar{q}q\rangle\langle\bar{q}Gq\rangle}(s) &= \frac{\langle\bar{s}s\rangle\langle\bar{q}g_s\sigma\cdot Gq\rangle+\langle\bar{q}q\rangle\langle\bar{s}g_s\sigma\cdot Gs\rangle}{48\pi^2}\\
&\quad+\frac{m_Qm_s\langle\bar{q}q\rangle\langle\bar{q}g_s\sigma\cdot Gq\rangle}{48\pi^2}\int_0^1d\alpha\left[\frac{2m_s^2}{\alpha^2}\delta'(s-\tilde{m}_Q^2)-\frac{1}{\alpha(1-\alpha)}\delta(s-\tilde{m}_Q^2)\right].
\end{aligned}
\tag{A3}
$$

in which

$$\alpha_{\max}=\frac{1}{2}\left[1+\frac{m_Q^2-m_s^2}{s}+\sqrt{\left(1+\frac{m_Q^2-m_s^2}{s}\right)^2-\frac{4m_Q^2}{s}}\right],\quad \alpha_{\min}=\frac{1}{2}\left[1+\frac{m_Q^2-m_s^2}{s}-\sqrt{\left(1+\frac{m_Q^2-m_s^2}{s}\right)^2-\frac{4m_Q^2}{s}}\right],$$
$$\beta_{\max}=\frac{m_s^2\alpha}{s\alpha-m_Q^2},\quad \beta_{\min}=1-\alpha,\quad \tilde{m}_Q^2=\frac{m_Q^2\alpha+m_s^2(1-\alpha)}{\alpha(1-\alpha)}. \tag{A4}$$

(ii) For the current $J_2(x)$ with $J^P=0^+$

$$\rho_2^{\rm pert}(s)=4\rho_1^{\rm pert}(s),\qquad \rho_2^{\langle\bar{q}q\rangle}(s)=8\rho_1^{\langle\bar{q}q\rangle}(s),\qquad \rho_2^{\langle\bar{s}s\rangle}(s)=4\rho_1^{\langle\bar{s}s\rangle}(s),$$
$$\rho_2^{\langle GG\rangle}(s)=\frac{\langle g_s^2GG\rangle}{256\pi^6}\int_{\alpha_{\min}}^{\alpha_{\max}}d\alpha\int_{\beta_{\min}}^{\beta_{\max}}d\beta\left[\left(\frac{m_Q^2}{\alpha^3}+\frac{m_s^2}{\beta^3}\right)\frac{(1-\alpha-\beta)^2(2\alpha m_s^2+2\beta m_Q^2-3\alpha\beta s)}{3}\right.$$
$$\left.-\left(\frac{1}{\alpha}+\frac{1}{\beta}\right)\frac{(1-\alpha-\beta)(\alpha m_s^2+\beta m_Q^2-\alpha\beta s)(\alpha m_s^2+\beta m_Q^2-2\alpha\beta s)}{\alpha\beta}\right],$$
$$\rho_2^{\langle\bar{q}Gq\rangle}(s)=\frac{\langle\bar{q}g_s\sigma\cdot Gq\rangle}{8\pi^4}\int_{\alpha_{\min}}^{\alpha_{\max}}d\alpha\int_{\beta_{\min}}^{\beta_{\max}}d\beta\left(\frac{m_Q}{\alpha}+\frac{m_s}{\beta}\right)(2\alpha m_s^2+2\beta m_Q^2-3\alpha\beta s),$$
$$\rho_2^{\langle\bar{q}q\rangle^2}(s)=\frac{4m_Qm_s\langle\bar{q}q\rangle^2}{3\pi^2}\sqrt{\left(1-\frac{m_Q^2-m_s^2}{s}\right)^2-\frac{4m_s^2}{s}}+\frac{\langle\bar{q}q\rangle\langle\bar{s}s\rangle(s-m_Q^2)(s-m_Qm_s-m_Q^2)}{3\pi^2s},$$
$$\rho_2^{\langle\bar{q}q\rangle\langle\bar{q}Gq\rangle}(s)=\frac{\langle\bar{s}s\rangle\langle\bar{q}g_s\sigma\cdot Gq\rangle+\langle\bar{q}q\rangle\langle\bar{s}g_s\sigma\cdot Gs\rangle}{6\pi^2}+\frac{2m_Qm_s^3\langle\bar{q}q\rangle\langle\bar{q}g_s\sigma\cdot Gq\rangle}{3\pi^2}\int_0^1d\alpha\frac{1}{\alpha^2}\delta'(s-\tilde{m}_Q^2). \tag{A5}$$

(iii) For the trace of current $J_{5\mu\nu}(x)$ with $J^P=0^+(\mathrm{T})$

$$\rho_3^{\rm pert}(s)=\frac{1}{4}\rho_1^{\rm pert}(s),\qquad \rho_3^{\langle\bar{q}q\rangle}(s)=\frac{1}{8}\rho_1^{\langle\bar{q}q\rangle}(s),\qquad \rho_3^{\langle\bar{s}s\rangle}(s)=\frac{1}{4}\rho_1^{\langle\bar{s}s\rangle}(s),$$
$$\rho_3^{\langle GG\rangle}(s)=\frac{\langle g_s^2GG\rangle}{4096\pi^6}\int_{\alpha_{\min}}^{\alpha_{\max}}d\alpha\int_{\beta_{\min}}^{\beta_{\max}}d\beta\left[\frac{(1-\beta)(\alpha m_s^2+\beta m_Q^2-\alpha\beta s)(\alpha m_s^2+\beta m_Q^2-2\alpha\beta s)}{4\alpha^2\beta}\right.$$
$$\left.+\frac{m_Q^2(1-\alpha-\beta)^2(2\alpha m_s^2+2\beta m_Q^2-3\alpha\beta s)}{3\alpha^3}\right],$$
$$\rho_3^{\langle\bar{q}Gq\rangle}(s)=\frac{\langle\bar{q}g_s\sigma\cdot Gq\rangle}{2048\pi^4}\int_{\alpha_{\min}}^{\alpha_{\max}}d\alpha\int_{\beta_{\min}}^{\beta_{\max}}d\beta(2\alpha m_s^2+2\beta m_Q^2-3\alpha\beta s)\left[3\left(\frac{m_Q}{\alpha}+\frac{m_s}{\beta}\right)+\frac{(m_Q-m_s)(1-\alpha-\beta)}{\alpha\beta}\right],$$
$$\rho_3^{\langle\bar{q}q\rangle^2}(s)=\frac{m_Qm_s\langle\bar{q}q\rangle^2}{48\pi^2}\sqrt{\left(1-\frac{m_Q^2-m_s^2}{s}\right)^2-\frac{4m_s^2}{s}}+\frac{\langle\bar{q}q\rangle\langle\bar{s}s\rangle(s-m_Q^2)(s-m_Qm_s-m_Q^2)}{192\pi^2s},$$
$$\rho_3^{\langle\bar{q}q\rangle\langle\bar{q}Gq\rangle}(s)=\frac{\langle\bar{s}s\rangle\langle\bar{q}g_s\sigma\cdot Gq\rangle}{384\pi^2}+\frac{\langle\bar{q}q\rangle\langle\bar{s}g_s\sigma\cdot Gs\rangle}{768\pi^2}+\frac{m_Q^2\langle\bar{q}q\rangle\langle\bar{s}g_s\sigma\cdot Gs\rangle}{1536\pi^2s}$$
$$+\frac{m_Qm_s\langle\bar{q}q\rangle\langle\bar{q}g_s\sigma\cdot Gq\rangle}{768\pi^2}\int_0^1d\alpha\left[\frac{8m_s^2}{\alpha^2}\delta'(s-\tilde{m}_Q^2)-\frac{1}{\alpha(1-\alpha)}\delta(s-\tilde{m}_Q^2)\right]. \tag{A6}$$

(iv) For the traceless symmetric part of the current $J_{5\mu\nu}(x)$ with $J^P = 0^+(\mathrm{S})$

$$\rho_4^{\mathrm{pert}}(s) = \frac{1}{128\pi^6}\int_{\alpha_{\min}}^{\alpha_{\max}} d\alpha \int_{\beta_{\min}}^{\beta_{\max}} d\beta (1-\alpha-\beta)^2(\alpha m_s^2+\beta m_Q^2-\alpha\beta s)^2\left[\frac{(1-\alpha-\beta)(\alpha m_s^2+\beta m_Q^2-5\alpha\beta s)^2}{8\alpha^3\beta^3}\right.$$
$$\left.-\frac{(1-\alpha-\beta)(\alpha m_s^2+\beta m_Q^2-\alpha\beta s)^2 s}{\alpha^2\beta^2}-\frac{(\alpha m_s^2+\beta m_Q^2-\alpha\beta s)(\alpha m_s^2+\beta m_Q^2-27\alpha\beta s)}{16\alpha^3\beta^3}\right],$$
$$\rho_4^{\langle\bar{q}q\rangle}(s) = -\frac{3\langle\bar{q}q\rangle}{128\pi^4}\int_{\alpha_{\min}}^{\alpha_{\max}} d\alpha \int_{\beta_{\min}}^{\beta_{\max}} d\beta\left(\frac{m_Q}{\alpha}+\frac{m_s}{\beta}\right)\frac{(1-\alpha-\beta)(\alpha m_s^2+\beta m_Q^2-\alpha\beta s)(\alpha m_s^2+\beta m_Q^2)}{\alpha\beta},$$
$$\rho_4^{\langle\bar{s}s\rangle}(s) = \frac{m_s\langle\bar{s}s\rangle(s-m_Q^2)(9s^4-45m_Q^2s^3-29m_Q^4s^2+7m_Q^6s-2m_Q^8)}{1536\pi^4 s^3}-\frac{5m_Q^4 m_s\langle\bar{s}s\rangle\log[m_Q^2/s]}{128\pi^4},$$
$$\rho_4^{\langle GG\rangle}(s) = \frac{\langle g_s^2GG\rangle}{1024\pi^6}\int_{\alpha_{\min}}^{\alpha_{\max}} d\alpha \int_{\beta_{\min}}^{\beta_{\max}} d\beta\left\{-\frac{(1-\alpha-\beta)(\alpha m_s^2+\beta m_Q^2-\alpha\beta s)(17\alpha m_s^2+17\beta m_Q^2-46\alpha\beta s)}{48\alpha^2\beta}\right.$$
$$+\frac{m_Q^2(1-\alpha-\beta)^2(2\alpha m_s^2+2\beta m_Q^2-3\alpha\beta s)}{4\alpha^3}-\frac{m_Q^2(1-\alpha-\beta)^3(\alpha m_s^2+\beta m_Q^2-3\alpha\beta s)}{3\alpha^3}$$
$$\left.+\frac{(1-\alpha-\beta)^2[9(\alpha m_s^2+\beta m_Q^2-\alpha\beta s)^2-78\alpha\beta s(\alpha m_s^2+\beta m_Q^2-\alpha\beta s)+28\alpha^2\beta^2 s^2]}{48\alpha^2\beta}\right\},$$
$$\rho_4^{\langle\bar{q}Gq\rangle}(s) = \frac{\langle\bar{q}g_s\sigma\cdot Gq\rangle}{2048\pi^4}\int_{\alpha_{\min}}^{\alpha_{\max}} d\alpha \int_{\beta_{\min}}^{\beta_{\max}} d\beta\left[\frac{m_s(70\alpha m_s^2+70\beta m_Q^2-27\alpha\beta s)}{3\beta}\right.$$
$$\left.-\frac{m_Q(1-\alpha-14\beta)(2\alpha m_s^2+2\beta m_Q^2-\alpha\beta s)}{\alpha\beta}+\frac{m_s(1-\alpha-\beta)(2\alpha m_s^2+2\beta m_Q^2-\alpha\beta s)}{\alpha\beta}\right],$$
$$\rho_4^{\langle\bar{q}q\rangle^2}(s) = \frac{m_Q m_s\langle\bar{q}q\rangle^2}{16\pi^2}\sqrt{\left(1-\frac{m_Q^2-m_s^2}{s}\right)^2-\frac{4m_s^2}{s}}$$
$$+\frac{\langle\bar{q}q\rangle\langle\bar{s}s\rangle(s-m_Q^2)(s^2-3m_Q m_s s-5m_Q^2 s+6m_Q^3 m_s+4m_Q^4)}{192\pi^2 s^2},$$
$$\rho_4^{\langle\bar{q}q\rangle\langle\bar{q}Gq\rangle}(s) = \frac{(14s^2-3m_Q^2 s-24m_Q^4)\langle\bar{q}q\rangle\langle\bar{s}g_s\sigma\cdot Gs\rangle}{1536\pi^2 s^2}+\frac{(s^2-2m_Q^4)\langle\bar{s}s\rangle\langle\bar{q}g_s\sigma\cdot Gq\rangle}{128\pi^2 s^2}$$
$$+\frac{m_Q m_s\langle\bar{q}q\rangle\langle\bar{q}g_s\sigma\cdot Gq\rangle}{768\pi^2}\int_0^1 d\alpha\left[\frac{24m_s^2}{\alpha^2}\delta'(s-\tilde{m}_Q^2)+\frac{1}{\alpha(1-\alpha)}\delta(s-\tilde{m}_Q^2)\right]. \tag{A7}$$

(v) For the current $J_{3\mu}(x)$ with $J^P = 1^+$

$$\rho_5^{\mathrm{pert}}(s) = \frac{1}{1024\pi^6}\int_{\alpha_{\min}}^{\alpha_{\max}} d\alpha \int_{\beta_{\min}}^{\beta_{\max}} d\beta\frac{(1-\alpha-\beta)^2(\alpha m_s^2+\beta m_Q^2-\alpha\beta s)^3(\alpha m_s^2+\beta m_Q^2-5\alpha\beta s)}{\alpha^3\beta^3},$$
$$\rho_5^{\langle\bar{q}q\rangle}(s) = -\frac{\langle\bar{q}q\rangle}{16\pi^4}\int_{\alpha_{\min}}^{\alpha_{\max}} d\alpha \int_{\beta_{\min}}^{\beta_{\max}} d\beta\left[\frac{m_Q(1-\alpha-\beta)(\alpha m_s^2+\beta m_Q^2-\alpha\beta s)(\alpha m_s^2+\beta m_Q^2-2\alpha\beta s)}{\alpha^2\beta}\right.$$
$$\left.+\frac{m_s(1-\alpha-\beta)(\alpha m_s^2+\beta m_Q^2-\alpha\beta s)(\alpha m_s^2+\beta m_Q^2-3\alpha\beta s)}{2\alpha\beta^2}\right],$$
$$\rho_5^{\langle\bar{s}s\rangle}(s) = \frac{m_s\langle\bar{s}s\rangle(s-m_Q^2)(3s^3-13m_Q^2 s^2-m_Q^4 s-m_Q^6)}{1536\pi^4 s^2}-\frac{m_Q^4 m_s\langle\bar{s}s\rangle\log[m_Q^2/s]}{128\pi^4},$$
$$\rho_5^{\langle GG\rangle}(s) = \frac{\langle g_s^2GG\rangle}{3072\pi^6}\int_{\alpha_{\min}}^{\alpha_{\max}} d\alpha \int_{\beta_{\min}}^{\beta_{\max}} d\beta\left\{\left(\frac{m_Q^2}{\alpha^3}+\frac{m_s^2}{\beta^3}\right)(1-\alpha-\beta)^2(\alpha m_s^2+\beta m_Q^2-2\alpha\beta s)\right.$$
$$\left.+\frac{(1-\alpha-\beta)(\alpha m_s^2+\beta m_Q^2-\alpha\beta s)}{2\alpha\beta}\left[\frac{3(\alpha m_s^2+\beta m_Q^2-3\alpha\beta s)}{\beta}-\frac{(3\alpha m_s^2+3\beta m_Q^2-5\alpha\beta s)}{\alpha}\right]\right\},$$

$$\rho_5^{\langle\bar{q}Gq\rangle}(s)=\frac{\langle\bar{q}g_s\sigma\cdot Gq\rangle}{64\pi^4}\int_{\alpha_{\min}}^{\alpha_{\max}}d\alpha\int_{\beta_{\min}}^{\beta_{\max}}d\beta\left[\frac{m_Q(2\alpha m_s^2+2\beta m_Q^2-3\alpha\beta s)}{\alpha}-\frac{m_s(1-\alpha-2\beta)(\alpha m_s^2+\beta m_Q^2-2\alpha\beta s)}{\beta^2}\right],$$

$$\rho_5^{\langle\bar{q}q\rangle^2}(s)=\frac{m_Q m_s\langle\bar{q}q\rangle^2}{12\pi^2}\sqrt{\left(1-\frac{m_Q^2-m_s^2}{s}\right)^2-\frac{4m_s^2}{s}}+\frac{\langle\bar{q}q\rangle\langle\bar{s}s\rangle(s-m_Q^2)(2s^2-3m_Q m_s s-m_Q^2 s-m_Q^4)}{72\pi^2 s^2},$$

$$\rho_5^{\langle\bar{q}q\rangle\langle\bar{q}Gq\rangle}(s)=\frac{(s^2+m_Q^4)(\langle\bar{s}s\rangle\langle\bar{q}g_s\sigma\cdot Gq\rangle+\langle\bar{q}q\rangle\langle\bar{s}g_s\sigma\cdot Gs\rangle)}{96\pi^2 s^2}+\frac{m_Q m_s\langle\bar{q}q\rangle\langle\bar{q}g_s\sigma\cdot Gq\rangle}{48\pi^2}\int_0^1 d\alpha\left[\frac{2m_s^2}{\alpha^2}\delta'(s-\tilde{m}_Q^2)-\frac{1}{\alpha}\delta(s-\tilde{m}_Q^2)\right]. \tag{A8}$$

(vi) For the current $J_{4\mu}(x)$ with $J^P=1^+$

$$\rho_6^{\rm pert}(s)=3\rho_5^{\rm pert}(s),\qquad \rho_6^{\langle\bar{s}s\rangle}(s)=3\rho_5^{\langle\bar{s}s\rangle}(s),$$

$$\rho_6^{\langle\bar{q}q\rangle}(s)=-\frac{3\langle\bar{q}q\rangle}{16\pi^4}\int_{\alpha_{\min}}^{\alpha_{\max}}d\alpha\int_{\beta_{\min}}^{\beta_{\max}}d\beta\left[\frac{m_Q(1-\alpha-\beta)(\alpha m_s^2+\beta m_Q^2-\alpha\beta s)(\alpha m_s^2+\beta m_Q^2-3\alpha\beta s)}{2\alpha^2\beta}+\frac{m_s(1-\alpha-\beta)(\alpha m_s^2+\beta m_Q^2-\alpha\beta s)(\alpha m_s^2+\beta m_Q^2-2\alpha\beta s)}{\alpha\beta^2}\right],$$

$$\rho_6^{\langle GG\rangle}(s)=-\frac{\langle g_s^2GG\rangle}{1024\pi^6}\int_{\alpha_{\min}}^{\alpha_{\max}}d\alpha\int_{\beta_{\min}}^{\beta_{\max}}d\beta\left\{\left(\frac{m_Q^2}{\alpha^3}+\frac{m_s^2}{\beta^3}\right)\frac{(1-\alpha-\beta)^2(\alpha m_s^2+\beta m_Q^2)}{3}+\frac{(1-\alpha-\beta)(\alpha m_s^2+\beta m_Q^2-\alpha\beta s)}{2\alpha\beta}\left[\frac{3\alpha m_s^2+3\beta m_Q^2-5\alpha\beta s}{\beta}-\frac{3\alpha m_s^2+3\beta m_Q^2-9\alpha\beta s}{\alpha}\right]\right\},$$

$$\rho_6^{\langle\bar{q}Gq\rangle}(s)=-\frac{3\langle\bar{q}g_s\sigma\cdot Gq\rangle}{64\pi^4}\int_{\alpha_{\min}}^{\alpha_{\max}}d\alpha\int_{\beta_{\min}}^{\beta_{\max}}d\beta\left[\frac{m_Q(1-2\alpha-\beta)(\alpha m_s^2+\beta m_Q^2-2\alpha\beta s)}{\alpha^2}+\frac{m_s(2\alpha m_s^2+2\beta m_Q^2-3\alpha\beta s)}{\beta}\right],$$

$$\rho_6^{\langle\bar{q}q\rangle^2}(s)=\frac{m_Q m_s\langle\bar{q}q\rangle^2}{4\pi^2}\sqrt{\left(1-\frac{m_Q^2-m_s^2}{s}\right)^2-\frac{4m_s^2}{s}}+\frac{\langle\bar{q}q\rangle\langle\bar{s}s\rangle(s-m_Q^2)(2s^2-m_Q m_s s-2m_Q^2 s-m_Q^3 m_s)}{16\pi^2 s^2},$$

$$\rho_6^{\langle\bar{q}q\rangle\langle\bar{q}Gq\rangle}(s)=\frac{\langle\bar{s}s\rangle\langle\bar{q}g_s\sigma\cdot Gq\rangle+\langle\bar{q}q\rangle\langle\bar{s}g_s\sigma\cdot Gs\rangle}{16\pi^2}+\frac{m_Q m_s\langle\bar{q}q\rangle\langle\bar{q}g_s\sigma\cdot Gq\rangle}{16\pi^2}\int_0^1 d\alpha\left[\frac{2m_s^2}{\alpha^2}\delta'(s-\tilde{m}_Q^2)-\frac{1}{\alpha}\delta(s-\tilde{m}_Q^2)\right]. \tag{A9}$$

(vii) For the traceless antisymmetric part of the current $J_{5\mu\nu}(x)$ with $J^P=1^+$(A)

$$\rho_7^{\rm pert}(s)=-\frac{3}{128\pi^6}\int_{\alpha_{\min}}^{\alpha_{\max}}d\alpha\int_{\beta_{\min}}^{\beta_{\max}}d\beta\frac{(1-\alpha-\beta)^2(\alpha m_s^2+\beta m_Q^2-\alpha\beta s)^3 s}{\alpha^2\beta^2},$$

$$\rho_7^{\langle\bar{q}q\rangle}(s)=-\frac{3\langle\bar{q}q\rangle}{16\pi^4}\int_{\alpha_{\min}}^{\alpha_{\max}}d\alpha\int_{\beta_{\min}}^{\beta_{\max}}d\beta\left(\frac{m_Q}{\alpha}+\frac{m_s}{\beta}\right)\frac{(1-\alpha-\beta)(\alpha m_s^2+\beta m_Q^2-\alpha\beta s)(\alpha m_s^2+\beta m_Q^2-3\alpha\beta s)}{\alpha\beta},$$

$$\rho_7^{\langle\bar{s}s\rangle}(s)=\frac{m_s\langle\bar{s}s\rangle(s-m_Q^2)^4}{128\pi^4 s^2},$$

$$\rho_7^{\langle GG\rangle}(s)=\frac{\langle g_s^2GG\rangle}{512\pi^6}\int_{\alpha_{\min}}^{\alpha_{\max}}d\alpha\int_{\beta_{\min}}^{\beta_{\max}}d\beta\Bigg[-\frac{(1-\alpha-\beta)(\alpha m_s^2+\beta m_Q^2-\alpha\beta s)(3\alpha m_s^2+3\beta m_Q^2-5\alpha\beta s)}{4\alpha^2\beta}$$
$$+\frac{(\alpha m_s^2+\beta m_Q^2-\alpha\beta s)(\alpha m_s^2+\beta m_Q^2-3\alpha\beta s)}{4\alpha\beta}-\frac{m_Q^2(1-\alpha-\beta)^2\beta s}{\alpha^2}\Bigg], \tag{A10}$$

$$\rho_7^{\langle\bar{q}Gq\rangle}(s)=\frac{\langle\bar{q}g_s\sigma\cdot Gq\rangle}{128\pi^4}\int_{\alpha_{\min}}^{\alpha_{\max}}d\alpha\int_{\beta_{\min}}^{\beta_{\max}}d\beta\Bigg[11(\alpha m_s^2+\beta m_Q^2-2\alpha\beta s)\left(\frac{m_Q}{\alpha}+\frac{m_s}{\beta}\right)$$
$$+\frac{(m_Q-m_s)(1-\alpha-\beta)(\alpha m_s^2+\beta m_Q^2-2\alpha\beta s)}{\alpha\beta}\Bigg],$$
$$\rho_7^{\langle\bar{q}q\rangle^2}(s)=\frac{m_Qm_s\langle\bar{q}q\rangle^2}{2\pi^2}\sqrt{\left(1-\frac{m_Q^2-m_s^2}{s}\right)^2-\frac{4m_s^2}{s}}$$
$$-\frac{\langle\bar{q}q\rangle\langle\bar{s}s\rangle(s-m_Q^2)(4s^2-3m_Qm_ss-2m_Q^2s-3m_Q^3m_s-2m_Q^4)}{24\pi^2s^2},$$
$$\rho_7^{\langle\bar{q}q\rangle\langle\bar{q}Gq\rangle}(s)=\frac{(5s^2+6m_Q^4)\langle\bar{q}q\rangle\langle\bar{s}g_s\sigma\cdot Gs\rangle}{96\pi^2s^2}+\frac{(s^2+m_Q^4)\langle\bar{s}s\rangle\langle\bar{q}g_s\sigma\cdot Gq\rangle}{16\pi^2s^2}$$
$$+\frac{m_Qm_s\langle\bar{q}q\rangle\langle\bar{q}g_s\sigma\cdot Gq\rangle}{96\pi^2}\int_0^1d\alpha\left[\frac{24m_s^2}{\alpha^2}\delta'(s-\tilde{m}_Q^2)-\frac{1}{\alpha(1-\alpha)}\delta(s-\tilde{m}_Q^2)\right]. \tag{A11}$$

(viii) For the traceless antisymmetric part of the current $J_{5\mu\nu}(x)$ with $J^P=1^-$(A)

$$\rho_8^{\rm pert}(s)=\rho_7^{\rm pert}(s),\qquad \rho_8^{\langle\bar{s}s\rangle}(s)=\rho_7^{\langle\bar{s}s\rangle}(s),$$
$$\rho_8^{\langle\bar{q}q\rangle}(s)=\frac{3\langle\bar{q}q\rangle}{16\pi^4}\int_{\alpha_{\min}}^{\alpha_{\max}}d\alpha\int_{\beta_{\min}}^{\beta_{\max}}d\beta\left(\frac{m_Q}{\alpha}+\frac{m_s}{\beta}\right)\frac{(1-\alpha-\beta)(\alpha m_s^2+\beta m_Q^2-\alpha\beta s)^2}{\alpha\beta},$$
$$\rho_8^{\langle GG\rangle}(s)=\frac{\langle g_s^2GG\rangle}{512\pi^6}\int_{\alpha_{\min}}^{\alpha_{\max}}d\alpha\int_{\beta_{\min}}^{\beta_{\max}}d\beta\Bigg[\frac{(1-\alpha-\beta)(\alpha m_s^2+\beta m_Q^2-\alpha\beta s)(3\alpha m_s^2+3\beta m_Q^2-7\alpha\beta s)}{4\alpha^2\beta}$$
$$-\frac{(\alpha m_s^2+\beta m_Q^2-\alpha\beta s)^2}{4\alpha\beta}-\frac{m_Q^2(1-\alpha-\beta)^2\beta s}{\alpha^2}\Bigg], \tag{A12}$$

$$\rho_8^{\langle\bar{q}Gq\rangle}(s)=-\frac{\langle\bar{q}g_s\sigma\cdot Gq\rangle}{128\pi^4}\int_{\alpha_{\min}}^{\alpha_{\max}}d\alpha\int_{\beta_{\min}}^{\beta_{\max}}d\beta\Bigg[11(\alpha m_s^2+\beta m_Q^2-2\alpha\beta s)\left(\frac{m_Q}{\alpha}+\frac{m_s}{\beta}\right)$$
$$+\frac{(m_Q-m_s)(1-\alpha-\beta)(\alpha m_s^2+\beta m_Q^2-\alpha\beta s)}{\alpha\beta}\Bigg],$$
$$\rho_8^{\langle\bar{q}q\rangle^2}(s)=-\frac{m_Qm_s\langle\bar{q}q\rangle^2}{2\pi^2}\sqrt{\left(1-\frac{m_Q^2-m_s^2}{s}\right)^2-\frac{4m_s^2}{s}}-\frac{\langle\bar{q}q\rangle\langle\bar{s}s\rangle(s-m_Q^2)^2(2s-3m_Qm_s-2m_Q^2)}{24\pi^2s^2},$$
$$\rho_8^{\langle\bar{q}q\rangle\langle\bar{q}Gq\rangle}(s)=-\frac{(s-m_Q^2)(5s+6m_Q^2)\langle\bar{q}q\rangle\langle\bar{s}g_s\sigma\cdot Gs\rangle}{96\pi^2s^2}-\frac{(s^2-m_Q^4)\langle\bar{s}s\rangle\langle\bar{q}g_s\sigma\cdot Gq\rangle}{16\pi^2s^2}$$
$$-\frac{m_Qm_s\langle\bar{q}q\rangle\langle\bar{q}g_s\sigma\cdot Gq\rangle}{96\pi^2}\int_0^1d\alpha\left[\frac{24m_s^2}{\alpha^2}\delta'(s-\tilde{m}_Q^2)-\frac{1}{\alpha(1-\alpha)}\delta(s-\tilde{m}_Q^2)\right]. \tag{A13}$$

(ix) For the traceless symmetric part of the current $J_{5\mu\nu}(x)$ with $J^P = 1^-(\mathrm{S})$

$$\begin{aligned}
\rho_9^{\mathrm{pert}}(s) &= -\frac{1}{64\pi^6}\int_{\alpha_{\min}}^{\alpha_{\max}} d\alpha \int_{\beta_{\min}}^{\beta_{\max}} d\beta \frac{(1-\alpha-\beta)^2(\alpha m_s^2+\beta m_Q^2-\alpha\beta s)^2(\alpha m_s^2+\beta m_Q^2-3\alpha\beta s)}{\alpha^2\beta^2} \\
&\quad\times\left[(1-\alpha-\beta)s+\frac{(\alpha m_s^2+\beta m_Q^2-\alpha\beta s)}{4\alpha\beta}\right], \\
\rho_9^{\langle\bar{q}q\rangle}(s) &= \rho_8^{\langle\bar{q}q\rangle}(s), \qquad \rho_9^{\langle\bar{q}q\rangle^2}(s) = \rho_8^{\langle\bar{q}q\rangle^2}(s), \\
\rho_9^{\langle\bar{s}s\rangle}(s) &= \frac{m_Q^2 m_s\langle\bar{s}s\rangle(s-m_Q^2)(3s-m_Q^2)(s^2+m_Q^2 s+m_Q^4)}{192\pi^4 s^3}+\frac{m_Q^4 m_s\langle\bar{s}s\rangle\log[m_Q^2/s]}{32\pi^4}, \\
\rho_9^{\langle GG\rangle}(s) &= \frac{\langle g_s^2 GG\rangle}{256\pi^6}\int_{\alpha_{\min}}^{\alpha_{\max}} d\alpha \int_{\beta_{\min}}^{\beta_{\max}} d\beta\left[\frac{(1-\alpha-\beta)(\alpha m_s^2+\beta m_Q^2-\alpha\beta s)(5\alpha m_s^2+5\beta m_Q^2-9\alpha\beta s)}{8\alpha^2\beta}\right. \\
&\quad-\frac{m_Q^2(1-\alpha-\beta)^2\beta s}{2\alpha^2}-\frac{m_Q^2(1-\alpha-\beta)^3(\alpha m_s^2+\beta m_Q^2-3\alpha\beta s)}{3\alpha^3} \\
&\quad\left.+\frac{(\alpha m_s^2+\beta m_Q^2-\alpha\beta s)^2}{8\alpha\beta}-\frac{(1-\alpha-\beta)^2(\alpha m_s^2+\beta m_Q^2-\alpha\beta s)(\alpha m_s^2+\beta m_Q^2-5\alpha\beta s)}{4\alpha^2\beta}\right], \\
\rho_9^{\langle\bar{q}Gq\rangle}(s) &= -\frac{\langle\bar{q}g_s\sigma\cdot Gq\rangle}{128\pi^4}\int_{\alpha_{\min}}^{\alpha_{\max}} d\alpha \int_{\beta_{\min}}^{\beta_{\max}} d\beta\left[13(\alpha m_s^2+\beta m_Q^2-2\alpha\beta s)\left(\frac{m_Q}{\alpha}+\frac{m_s}{\beta}\right)\right. \\
&\quad\left.-\frac{(m_Q-m_s)(1-\alpha-\beta)(\alpha m_s^2+\beta m_Q^2-\alpha\beta s)}{\alpha\beta}\right], \\
\rho_9^{\langle\bar{q}q\rangle\langle\bar{q}Gq\rangle}(s) &= -\frac{(s-m_Q^2)(7s+6m_Q^2)\langle\bar{q}q\rangle\langle\bar{s}g_s\sigma\cdot Gs\rangle}{96\pi^2 s^2}-\frac{(s^2-m_Q^4)\langle\bar{s}s\rangle\langle\bar{q}g_s\sigma\cdot Gq\rangle}{16\pi^2 s^2} \\
&\quad-\frac{m_Q m_s\langle\bar{q}q\rangle\langle\bar{q}g_s\sigma\cdot Gq\rangle}{96\pi^2}\int_0^1 d\alpha\left[\frac{24m_s^2}{\alpha^2}\delta'(s-\tilde{m}_Q^2)+\frac{1}{\alpha(1-\alpha)}\delta(s-\tilde{m}_Q^2)\right].
\end{aligned} \tag{A14}$$

(x) For the traceless symmetric part of the current $J_{5\mu\nu}(x)$ with $J^P = 2^+(\mathrm{S})$

$$\begin{aligned}
\rho_{10}^{\mathrm{pert}}(s) &= \frac{1}{96\pi^6}\int_{\alpha_{\min}}^{\alpha_{\max}} d\alpha \int_{\beta_{\min}}^{\beta_{\max}} d\beta \frac{(1-\alpha-\beta)^2(\alpha m_s^2+\beta m_Q^2-\alpha\beta s)^2}{\alpha^2\beta^2} \\
&\quad\times\left[\frac{(1-\alpha-\beta)(\alpha m_s^2+\beta m_Q^2-5\alpha\beta s)^2}{8\alpha\beta}+\frac{(\alpha m_s^2+\beta m_Q^2-\alpha\beta s)(2\alpha m_s^2+2\beta m_Q^2-9\alpha\beta s)}{4\alpha\beta}\right. \\
&\quad\left.-(1-\alpha-\beta)(\alpha m_s^2+\beta m_Q^2-\alpha\beta s)s\right], \\
\rho_{10}^{\langle\bar{q}q\rangle}(s) &= \frac{5}{3}\rho_7^{\langle\bar{q}q\rangle}(s), \qquad \rho_9^{\langle\bar{q}q\rangle^2}(s) = \rho_8^{\langle\bar{q}q\rangle^2}(s), \\
\rho_{10}^{\langle\bar{s}s\rangle}(s) &= \frac{m_s\langle\bar{s}s\rangle(s-m_Q^2)(9s^4-36m_Q^2 s^3-m_Q^4 s^2-m_Q^6 s-m_Q^8)}{576\pi^4 s^3}-\frac{5m_Q^4 m_s\langle\bar{s}s\rangle\log[m_Q^2/s]}{96\pi^4}, \\
\rho_{10}^{\langle GG\rangle}(s) &= \frac{\langle g_s^2 GG\rangle}{768\pi^6}\int_{\alpha_{\min}}^{\alpha_{\max}} d\alpha \int_{\beta_{\min}}^{\beta_{\max}} d\beta\left[-\frac{(1-\alpha-\beta)(\alpha m_s^2+\beta m_Q^2-\alpha\beta s)(17\alpha m_s^2+17\beta m_Q^2-47\alpha\beta s)}{8\alpha^2\beta}\right. \\
&\quad+\frac{m_Q^2(1-\alpha-\beta)^2(4\alpha m_s^2+4\beta m_Q^2-9\alpha\beta s)}{2\alpha^3}-\frac{m_Q^2(1-\alpha-\beta)^3(\alpha m_s^2+\beta m_Q^2-3\alpha\beta s)}{3\alpha^3} \\
&\quad-\frac{5(\alpha m_s^2+\beta m_Q^2-\alpha\beta s)(\alpha m_s^2+\beta m_Q^2-3\alpha\beta s)}{8\alpha\beta}+\frac{(1-\alpha-\beta)^2(\alpha m_s^2+\beta m_Q^2-\alpha\beta s)s}{\alpha} \\
&\quad\left.-\frac{(1-\alpha-\beta)^2(\alpha m_s^2+\beta m_Q^2-\alpha\beta s)^2}{4\alpha^2\beta}\right],
\end{aligned}$$

$$\rho_{10}^{\langle\bar{q}Gq\rangle}(s)=\frac{5\langle\bar{q}g_s\sigma\cdot Gq\rangle}{384\pi^4}\int_{\alpha_{\min}}^{\alpha_{\max}}d\alpha\int_{\beta_{\min}}^{\beta_{\max}}d\beta\Bigg[13(\alpha m_s^2+\beta m_Q^2-2\alpha\beta s)\left(\frac{m_Q}{\alpha}+\frac{m_s}{\beta}\right)-\frac{(m_Q-m_s)(1-\alpha-\beta)(\alpha m_s^2+\beta m_Q^2-2\alpha\beta s)}{\alpha\beta}\Bigg],$$

$$\rho_{10}^{\langle\bar{q}q\rangle\langle\bar{q}Gq\rangle}(s)=\frac{5(7s^2+6m_Q^4)\langle\bar{q}q\rangle\langle\bar{s}g_s\sigma\cdot Gs\rangle}{288\pi^2s^2}+\frac{5(s^2+m_Q^4)\langle\bar{s}s\rangle\langle\bar{q}g_s\sigma\cdot Gq\rangle}{48\pi^2s^2}+\frac{5m_Qm_s\langle\bar{q}q\rangle\langle\bar{q}g_s\sigma\cdot Gq\rangle}{288\pi^2}\int_0^1d\alpha\left[\frac{24m_s^2}{\alpha^2}\delta'(s-\tilde{m}_Q^2)+\frac{1}{\alpha(1-\alpha)}\delta(s-\tilde{m}_Q^2)\right].\tag{A15}$$

(xi) For the current $J_{3\mu}(x)$ with $J^P=0^-$

$$\rho_{11}^{\rm pert}(s)=-\frac{1}{1024\pi^6}\int_{\alpha_{\min}}^{\alpha_{\max}}d\alpha\int_{\beta_{\min}}^{\beta_{\max}}d\beta\frac{(1-\alpha-\beta)^2(\alpha m_s^2+\beta m_Q^2-\alpha\beta s)^3(\alpha m_s^2+\beta m_Q^2+3\alpha\beta s)}{\alpha^3\beta^3},$$

$$\rho_{11}^{\langle\bar{q}q\rangle}(s)=\frac{\langle\bar{q}q\rangle}{16\pi^4}\int_{\alpha_{\min}}^{\alpha_{\max}}d\alpha\int_{\beta_{\min}}^{\beta_{\max}}d\beta\Bigg[\frac{m_Q(1-\alpha-\beta)(\alpha m_s^2+\beta m_Q^2-\alpha\beta s)(\alpha m_s^2+\beta m_Q^2-2\alpha\beta s)}{\alpha^2\beta}+\frac{m_s(1-\alpha-\beta)(\alpha m_s^2+\beta m_Q^2-\alpha\beta s)(\alpha m_s^2+\beta m_Q^2+\alpha\beta s)}{2\alpha\beta^2}\Bigg],$$

$$\rho_{11}^{\langle\bar{s}s\rangle}(s)=\frac{m_s\langle\bar{s}s\rangle(s-m_Q^2)(s^3+m_Q^2s^2+13m_Q^4s-3m_Q^6)}{1536\pi^4s^2}+\frac{m_Q^4m_s\langle\bar{s}s\rangle\log[m_Q^2/s]}{128\pi^4},$$

$$\rho_{11}^{\langle GG\rangle}(s)=-\frac{\langle g_s^2GG\rangle}{1024\pi^6}\int_{\alpha_{\min}}^{\alpha_{\max}}d\alpha\int_{\beta_{\min}}^{\beta_{\max}}d\beta\Bigg\{\frac{(1-\alpha-\beta)^2(\alpha m_s^2+\beta m_Q^2)}{3}\left(\frac{m_Q^2}{\alpha^3}+\frac{m_s^2}{\beta^3}\right)-\frac{(1-\alpha-\beta)(\alpha m_s^2+\beta m_Q^2-\alpha\beta s)}{2\alpha\beta}\left[\frac{\alpha m_s^2+\beta m_Q^2-3\alpha\beta s}{\alpha}-\frac{\alpha m_s^2+\beta m_Q^2+\alpha\beta s}{\beta}\right]\Bigg\},$$

$$\rho_{11}^{\langle\bar{q}Gq\rangle}(s)=\frac{\langle\bar{q}g_s\sigma\cdot Gq\rangle}{64\pi^4}\int_{\alpha_{\min}}^{\alpha_{\max}}d\alpha\int_{\beta_{\min}}^{\beta_{\max}}d\beta\Bigg[\frac{m_s(1-\alpha-2\beta)(\alpha m_s^2+\beta m_Q^2)}{\beta^2}-\frac{m_Q(2\alpha m_s^2+2\beta m_Q^2-3\alpha\beta s)}{\alpha}\Bigg],$$

$$\rho_{11}^{\langle\bar{q}q\rangle^2}(s)=-\frac{m_Qm_s\langle\bar{q}q\rangle^2}{12\pi^2}\sqrt{\left(1-\frac{m_Q^2-m_s^2}{s}\right)^2-\frac{4m_s^2}{s}}+\frac{m_Q\langle\bar{q}q\rangle\langle\bar{s}s\rangle(s-m_Q^2)(m_Ss+m_Qs-m_Q^3)}{24\pi^2s^2},$$

$$\rho_{11}^{\langle\bar{q}q\rangle\langle\bar{q}Gq\rangle}(s)=-\frac{(s^2-3m_Q^4)(\langle\bar{s}s\rangle\langle\bar{q}g_s\sigma\cdot Gq\rangle+\langle\bar{q}q\rangle\langle\bar{s}g_s\sigma\cdot Gs\rangle)}{96\pi^2s^2}-\frac{m_Qm_s\langle\bar{q}q\rangle\langle\bar{q}g_s\sigma\cdot Gq\rangle}{48\pi^2}\int_0^1d\alpha\left[\frac{2m_s^2}{\alpha^2}\delta'(s-\tilde{m}_Q^2)-\frac{1}{\alpha}\delta(s-\tilde{m}_Q^2)\right].\tag{A16}$$

(xii) For the current $J_{4\mu}(x)$ with $J^P=0^-$

$$\rho_{12}^{\rm pert}(s)=\rho_{11}^{\rm pert}(s),\qquad\rho_{12}^{\langle\bar{s}s\rangle}(s)=\rho_{11}^{\langle\bar{s}s\rangle}(s),$$

$$\rho_{12}^{\langle\bar{q}q\rangle}(s)=\frac{\langle\bar{q}q\rangle}{16\pi^4}\int_{\alpha_{\min}}^{\alpha_{\max}}d\alpha\int_{\beta_{\min}}^{\beta_{\max}}d\beta\Bigg[\frac{m_Q(1-\alpha-\beta)(\alpha m_s^2+\beta m_Q^2-\alpha\beta s)(\alpha m_s^2+\beta m_Q^2+\alpha\beta s)}{2\alpha^2\beta}+\frac{m_s(1-\alpha-\beta)(\alpha m_s^2+\beta m_Q^2-\alpha\beta s)(\alpha m_s^2+\beta m_Q^2-2\alpha\beta s)}{\alpha\beta^2}\Bigg],$$

$$\rho_{12}^{\langle GG\rangle}(s) = -\frac{\langle g_s^2 GG\rangle}{1024\pi^6}\int_{\alpha_{\min}}^{\alpha_{\max}} d\alpha \int_{\beta_{\min}}^{\beta_{\max}} d\beta \left\{ \frac{(1-\alpha-\beta)^2(\alpha m_s^2+\beta m_Q^2)}{3}\left(\frac{m_Q^2}{\alpha^3}+\frac{m_s^2}{\beta^3}\right) - \frac{(1-\alpha-\beta)(\alpha m_s^2+\beta m_Q^2-\alpha\beta s)}{2\alpha\beta}\left[\frac{\alpha m_s^2+\beta m_Q^2-3\alpha\beta s}{\beta}-\frac{\alpha m_s^2+\beta m_Q^2+\alpha\beta s}{\alpha}\right]\right\},$$

$$\rho_{12}^{\langle \bar{q}Gq\rangle}(s) = \frac{\langle \bar{q}g_s\sigma\cdot Gq\rangle}{64\pi^4}\int_{\alpha_{\min}}^{\alpha_{\max}} d\alpha \int_{\beta_{\min}}^{\beta_{\max}} d\beta \left[\frac{m_Q(1-2\alpha-\beta)(\alpha m_s^2+\beta m_Q^2)}{\alpha^2} - \frac{m_s(2\alpha m_s^2+2\beta m_Q^2-3\alpha\beta s)}{\beta}\right],$$

$$\rho_{12}^{\langle \bar{q}q\rangle^2}(s) = -\frac{m_Q m_s\langle\bar{q}q\rangle^2}{12\pi^2}\sqrt{\left(1-\frac{m_Q^2-m_s^2}{s}\right)^2-\frac{4m_s^2}{s}} - \frac{\langle\bar{q}q\rangle\langle\bar{s}s\rangle(s-m_Q^2)(2s^2-m_Q m_s s-2m_Q^2 s+3m_Q^3 m_s)}{48\pi^2 s^2},$$

$$\rho_{12}^{\langle \bar{q}q\rangle\langle\bar{q}Gq\rangle}(s) = -\frac{\langle\bar{s}s\rangle\langle\bar{q}g_s\sigma\cdot Gq\rangle+\langle\bar{q}q\rangle\langle\bar{s}g_s\sigma\cdot Gs\rangle}{48\pi^2} - \frac{m_Q m_s\langle\bar{q}q\rangle\langle\bar{q}g_s\sigma\cdot Gq\rangle}{48\pi^2}\int_0^1 d\alpha\left[\frac{2m_s^2}{\alpha^2}\delta'(s-\tilde{m}_Q^2)-\frac{1}{\alpha}\delta(s-\tilde{m}_Q^2)\right]. \quad \text{(A17)}$$

[1] C. Patrignani *et al.* (Particle Data Group), Chin. Phys. C **40**, 100001 (2016).
[2] R. Aaij *et al.* (LHCb Collaboration), Phys. Rev. Lett. **115**, 072001 (2015).
[3] E. Klempt and A. Zaitsev, Phys. Rep. **454**, 1 (2007).
[4] H.-X. Chen, W. Chen, X. Liu, and S.-L. Zhu, Phys. Rep. **639**, 1 (2016).
[5] A. Esposito, A. L. Guerrieri, F. Piccinini, A. Pilloni, and A. D. Polosa, Int. J. Mod. Phys. A **30**, 1530002 (2015).
[6] S. L. Olsen, Front. Phys. **10**, 121 (2015).
[7] R. F. Lebed, R. E. Mitchell, and E. S. Swanson, Prog. Part. Nucl. Phys. **93**, 143 (2017).
[8] V. M. Abazov *et al.* (D0 Collaboration), Phys. Rev. Lett. **117**, 022003 (2016).
[9] R. Aaij *et al.* (LHCb Collaboration), Phys. Rev. Lett. **117**, 152003 (2016).
[10] The CMS Collaboration, Report No. CMS-PAS-BPH-16-002, 2016.
[11] The D0 Collaboration, http://indico.cern.ch/event/432527/contributions/1072024/ (2016).
[12] W. Chen, H.-X. Chen, X. Liu, T. G. Steele, and S.-L. Zhu, Phys. Rev. Lett. **117**, 022002 (2016).
[13] S. S. Agaev, K. Azizi, and H. Sundu, Phys. Rev. D **93**, 074024 (2016).
[14] C. M. Zanetti, M. Nielsen, and K. P. Khemchandani, Phys. Rev. D **93**, 096011 (2016).
[15] Z.-G. Wang, Commun. Theor. Phys. **66**, 335 (2016).
[16] Z.-G. Wang, Eur. Phys. J. C **76**, 279 (2016).
[17] W. Wang and R. Zhu, Chin. Phys. C **40**, 093101 (2016).
[18] L. Tang and C.-F. Qiao, Eur. Phys. J. C **76**, 558 (2016).
[19] S. S. Agaev, K. Azizi, and H. Sundu, Phys. Rev. D **93**, 114007 (2016).
[20] J. M. Dias, K. P. Khemchandani, A. Martnez Torres, M. Nielsen, and C. M. Zanetti, Phys. Lett. B **758**, 235 (2016).
[21] R. Albuquerque, S. Narison, A. Rabemananjara, and D. Rabetiarivony, Int. J. Mod. Phys. A **31**, 1650093 (2016).
[22] Y.-R. Liu, X. Liu, and S.-L. Zhu, Phys. Rev. D **93**, 074023 (2016).
[23] F. Stancu, J. Phys. G **43**, 105001 (2016).
[24] A. Ali, L. Maiani, A. D. Polosa, and V. Riquer, Phys. Rev. D **94**, 034036 (2016).
[25] X.-G. He and P. Ko, Phys. Lett. B **761**, 92 (2016).
[26] T. J. Burns and E. S. Swanson, Phys. Lett. B **760**, 627 (2016).
[27] F.-K. Guo, U.-G. Meiner, and B.-S. Zou, Commun. Theor. Phys. **65**, 593 (2016).
[28] Q.-F. L and Y.-B. Dong, Phys. Rev. D **94**, 094041 (2016).
[29] F. Goerke, T. Gutsche, M. A. Ivanov, J. G. Korner, V. E. Lyubovitskij, and P. Santorelli, Phys. Rev. D **94**, 094017 (2016).
[30] A. K. Agamaliev, T. M. Aliev, and M. Savc, Phys. Rev. D **95**, 036015 (2017).
[31] S. S. Agaev, K. Azizi, and H. Sundu, Eur. Phys. J. Plus **131**, 351 (2016).
[32] X.-W. Kang and J. A. Oller, Phys. Rev. D **94**, 054010 (2016).
[33] X. Chen and J. Ping, Eur. Phys. J. C **76**, 351 (2016).
[34] M. Albaladejo, J. Nieves, E. Oset, Z.-F. Sun, and X. Liu, Phys. Lett. B **757**, 515 (2016).
[35] C. B. Lang, D. Mohler, and S. Prelovsek, Phys. Rev. D **94**, 074509 (2016).
[36] R. Chen and X. Liu, Phys. Rev. D **94**, 034006 (2016).
[37] J.-X. Lu, X.-L. Ren, and L.-S. Geng, Eur. Phys. J. C **77**, 94 (2017).

[38] B.-X. Sun, F.-Y. Dong, and J.-R. Pang, Chin. Phys. C **41**, 074104 (2017).
[39] X.-H. Liu and G. Li, Eur. Phys. J. C **76**, 455 (2016).
[40] A. Esposito, A. Pilloni, and A. D. Polosa, Phys. Lett. B **758**, 292 (2016).
[41] H.-X. Chen, W. Chen, X. Liu, Y.-R. Liu, and S.-L. Zhu, Rep. Prog. Phys. **80**, 076201 (2017).
[42] B. Aubert *et al.* (*BABAR* Collaboration), Phys. Rev. Lett. **90**, 242001 (2003).
[43] D. Besson *et al.* (CLEO Collaboration), Phys. Rev. D **68**, 032002 (2003); **75**, 119908 (2007).
[44] S. Godfrey and R. Kokoski, Phys. Rev. D **43**, 1679 (1991).
[45] T. Barnes, F. E. Close, and H. J. Lipkin, Phys. Rev. D **68**, 054006 (2003).
[46] Y.-Q. Chen and X.-Q. Li, Phys. Rev. Lett. **93**, 232001 (2004).
[47] M. A. Shifman, A. I. Vainshtein, and V. I. Zakharov, Nucl. Phys. **B147**, 385 (1979).
[48] L. J. Reinders, H. Rubinstein, and S. Yazaki, Phys. Rep. **127**, 1 (1985).
[49] P. Colangelo and A. Khodjamirian, *At the Frontier of Particle Physics (Handbook of QCD)* Vol. 3 (World Scientific, Singapore, 2001).
[50] R. Jaffe, Phys. Rep. **409**, 1 (2005).
[51] M.-L. Du, W. Chen, X.-L. Chen, and S.-L. Zhu, Phys. Rev. D **87**, 014003 (2013).
[52] W. Chen, T. Steele, and S.-L. Zhu, Phys. Rev. D **89**, 054037 (2014).
[53] W. Chen and S.-L. Zhu, Phys. Rev. D **83**, 034010 (2011).
[54] W. Chen and S.-L. Zhu, Phys. Rev. D **81**, 105018 (2010).
[55] J. Govaerts, L. J. Reinders, P. Francken, X. Gonze, and J. Weyers, Nucl. Phys. **B284**, 674 (1987).
[56] S. Narison, Phys. Lett. B **707**, 259 (2012).
[57] J. H. Kuhn, M. Steinhauser, and C. Sturm, Nucl. Phys. **B778**, 192 (2007).